

## ABSTRACT

Rodney C. Hill. CHARACTERIZATION AND DIFFERENTIATION OF NALM-6 AND JURKAT CELL LINES USING CONFOCAL LASER SCANNING MICROSCOPY.

Department of Biology, December 2009.

Confocal microscopy is an optical imaging technique that gives the ability to examine a single biological cell in three-dimensions by constructing image “slices” of the different layers of the cell. It allows users to examine different aspects of cellular morphology and processes, and has extreme research potential for biological application. Laser scanning confocal microscopy has proved to be most suitable for the analysis of structural details of thick specimens, and promises to be of great potential in providing 3-D volume renderings of living cells or tissues (Singh 1998). Leukemia is cancer of blood forming tissues, characterized by overcrowding of healthy blood cells by abnormal, cancerous blood cells. Diagnosis of leukemia usually consists of pathologic examination of bone marrow or blood, cytogenetics, and/or molecular analysis of DNA/RNA. While confocal microscopy has been applied to study some aspects of cancerous cells, it has not been used to differentiate between types of cancerous cells. This study focuses on applying confocal microscopy as a differentiative tool for comparing leukemic and non-leukemic cell lines. By fluorescently staining the nuclei and mitochondria of the cells of interest prior to imaging, these areas in the cell are visible during imaging. It was anticipated that with the nuclear and mitochondrial staining, morphological differences would be found between different acute lymphoid leukemia (ALL) cell lines, ALL patient blood cells, and non-leukemic donor blood cells. Acute myeloid leukemia (AML) cell lines and AML patient blood samples were also imaged for further examination. The results of this study suggest that confocal microscopy is capable of detecting morphological differences between different types of leukemic cells.

CHARACTERIZATION AND DIFFERENTIATION OF NALM-6 AND JURKAT  
CELL LINES USING CONFOCAL LASER SCANNING MICROSCOPY

A thesis  
Presented to  
The Faculty of the Department of Biology  
East Carolina University

In partial fulfillment  
of the Requirements for the Degree  
Master of Science in Molecular Biology/Biotechnology

Rodney Chason Hill  
December 2009



December 2009

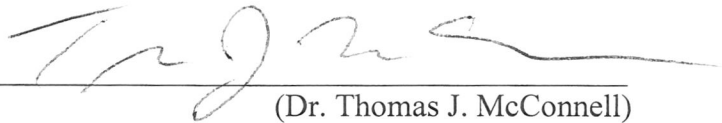
CHARACTERIZATION AND DIFFERENTIATION OF NALM-6 AND JURKAT  
CELL LINES USING CONFOCAL LASER SCANNING MICROSCOPY

By

Rodney C. Hill

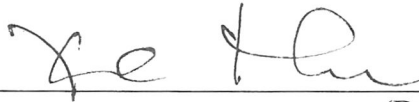
APPROVED BY:

DIRECTOR OF THESIS: \_\_\_\_\_



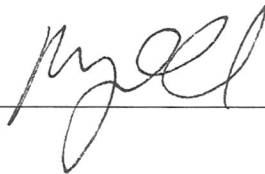
(Dr. Thomas J. McConnell)

COMMITTEE MEMBER: \_\_\_\_\_



(Dr. Xin-Hua Hu)

COMMITTEE MEMBER: \_\_\_\_\_



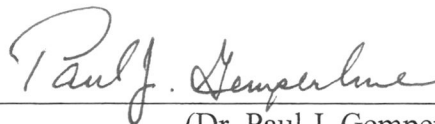
(Dr. Mary A. Farwell)

CHAIR OF THE DEPARTMENT OF BIOLOGY: \_\_\_\_\_



(Dr. Jeffrey S. McKinnon)

DEAN OF THE GRADUATE SCHOOL: \_\_\_\_\_



(Dr. Paul J. Gemperline)

## **DEDICATION**

I would like to extend my deepest gratitude to my wife Jenna, for she has been extremely patient and supportive throughout this whole project. Her love and encouragement have helped motivate me to pursue and complete my goal of attaining a Master's degree. I would also like to thank my parents and family for their love and support of my education.

## **ACKNOWLEDGEMENTS**

I would like to thank my committee members, Dr. McConnell, Dr. Hu, and Dr. Farwell for all of their help and contributions throughout the course this project. I am very grateful for their dedication to see me succeed. It is because of their guidance that I was able to take on and complete this project. I would also like to thank Dr. Weidner for his help and for allowing me to use the confocal microscopy facilities. I would like to thank Dr. Burke and Dr. Wiley as well, along with their staff, whose efforts helped to make this project whole.

## TABLE OF CONTENTS

LIST OF TABLES .....	vi
LIST OF FIGURES .....	vii
INTRODUCTION.....	1
Leukemia.....	1
Overview.....	1
Types.....	1
Diagnosis.....	3
Treatments.....	4
Leukemic Cell Lines.....	5
Confocal Laser Scanning Microscopy .....	6
Overview.....	6
Confocal Imaging.....	7
Experimental Cell Lines.....	8
NALM-6.....	8
Jurkat.....	9
U937.....	9
HL60.....	10
MATERIALS AND METHODS.....	11
Cell Lines.....	11
Cell Preparation from blood samples.....	11
Cell Staining.....	13
Confocal Imaging.....	14

Comparison of Cell Images.....	14
RESULTS.....	21
DISCUSSION.....	39
CONCLUSIONS.....	43
REFERENCES.....	45
APPENDIX A. MINIMUM ESSENTIAL MEDIUM (MEM) .....	49
APPENDIX B. RPMI MEDIUM .....	50
APPENDIX C. REPRESENTATIVE IMAGES COLLECTED OF EACH CELL TYPE..	51

## LIST OF TABLES

<u>Table 1</u> : Cell Information Table.....	13
<u>Table 2</u> : Morphological Definitions.....	15
<u>Table 3</u> : Results taken from NALM-6 confocal images.....	25
<u>Table 4</u> : Results taken from Jurkat confocal images.....	26
<u>Table 5</u> : Results taken from PHA stimulated non-leukemic T-cell confocal images.....	27
<u>Table 6</u> : Results taken from TPA stimulated non-leukemic B-cell confocal images.....	28
<u>Table 7</u> : Results taken from HL-60 confocal images.....	29
<u>Table 8</u> : Results taken from U937 confocal images.....	30
<u>Table 9</u> : Results taken from Patient #1 (ALL) confocal images.....	31
<u>Table 10</u> : Results taken from Patient #2 (AML) confocal images.....	32
<u>Table 11</u> : Results taken from Patient #3 (Undiagnosed) confocal images.....	33
<u>Table 12</u> : Results taken from Patient #4 (AML) confocal images.....	34
<u>Table 13</u> : Results taken from Patient #5 (AML) confocal images.....	35
<u>Table 14</u> : Results taken from Patient #6 (ALL) confocal images.....	36
<u>Table 15</u> : Summary of results.....	37

## LIST OF FIGURES

<u>Figure 1</u> : Schematic of a confocal laser scanning microscope.....	7
<u>Figure 2</u> : Overall cell morphology.....	16
<u>Figure 3</u> : Cell measurement.....	17
<u>Figure 4</u> : Nuclear morphology.....	19
<u>Figure 5</u> : Mitochondrial distribution.....	20

## INTRODUCTION

### Leukemia

**Overview.** Leukemia is a cancerous disorder of blood-forming tissue, specifically bone marrow, that is characterized by uncontrolled proliferation of leukocytes. Abnormal white blood cells undergo uncontrolled proliferation, therefore crowding out the normal cells found in the bone marrow (Griffiths 1999). Cells that may be affected include healthy white blood cells, red blood cells, and platelets. As a result, leukemia patients can show symptoms such as immunodeficiency, anemia, and other related symptoms such as bone pain, headaches, and nausea. The production of normal blood cells is not increased to make up for the anemia, granulocytopenia, and thrombocytopenia that can develop, apparently because the leukemic cells somehow interfere with the proliferation and/or differentiation of normal stem cells (Clarkson 1967). The initial events that cause leukemia are not known. However, recent evidence suggests that most leukemogenic mutations occur in stem cells or their immediate progeny, causing them to become leukemic stem cells that are responsible for the initial development and maintenance of cancerous cells (Anderson 2001). The mechanism by which leukemic cells interfere with normal hematopoiesis remains unclear (Guilloton 2005).

**Types.** There are four major kinds of leukemia, divided into two types based on how quickly they progress. Acute leukemia progresses rapidly and requires immediate treatment. Immature white blood cells build up very rapidly and crowd out the normal, healthy bone marrow cells. The major reason leukemic cells displace normal hematopoietic precursors in acute leukemia is that they largely fail to differentiate and continue to proliferate (Clarkson 1967). These hematopoietic stem cells don't develop or mature properly, and as a result they either lose apoptotic control or lose proliferative regulation. Acute leukemia is further divided

into acute myeloid leukemia (AML) and acute lymphoid leukemia (ALL), depending on the lineage precursors of the leukemic cells. AML is cancer of myeloid progenitor cells. These cells would normally differentiate into erythrocytes, platelets, basophils, eosinophils, neutrophils or monocytes. ALL is cancer of lymphoid progenitor cells, which under normal circumstances would differentiate into T lymphocytes, B lymphocytes, or natural killer cells (Bartholdy 2004). The NALM-6 cell line used in these thesis experiments is an established human B cell precursor ALL cell line. The establishment of malignant cell lines from leukemia patients, such as NALM-6, has allowed for a more thorough investigation of the genetics, biochemistry, and immunology of leukemic cells (LeBien 1982). Blast cells from the bone marrow of AML and ALL patients will also be examined in this study.

Chronic leukemia progresses slowly and can go undetected, sometimes taking years to present. It occurs mainly in adults, rarely in children, and accounts for more than 20,000 new cases of leukemia per year. Chronic leukemia, unlike acute leukemia, is characterized by the buildup of somewhat mature, but still abnormal, white blood cells. These abnormal cells still have some function early in the disease, but they proliferate more rapidly than normal blood cells, and eventually crowd out the normal cells. Chronic leukemia, like acute leukemia, is also further classified by the lineage of the cell, with chronic myeloid leukemia (CML), and chronic lymphoid leukemia (CLL). CML is associated with an abnormality in the Philadelphia chromosome, which contains the BCR-ABL gene, responsible for producing an abnormal protein called tyrosine kinase. Abnormal activation of tyrosine kinases or the signaling pathways they control is thought to play a critical role in the neoplastic process of many human malignancies (Wadleigh 2005). In most CLL cases, the cells of origin are clonal B cells trapped in the B-cell differentiation pathway.

**Diagnosis.** Current methods of diagnosis include pathologic examination of bone marrow, peripheral blood or lymphoid tissue, blood cell counts via flow cytometry, cytogenetics, and molecular analysis of DNA/RNA. It has been acknowledged that diagnostic cytogenetics provides one of the most valuable prognostic indicators in AML (Grimwade 1998). The correct diagnosis of the type of leukemia is crucial for treatment planning.

Once a patient has been diagnosed with an acute leukemia, further classification of the disease can be made in part by looking at morphological characteristics of a patient's blast cells. The French-American-British (FAB) classification of acute leukemias is used to further categorize ALL or AML on the basis of cell morphology, determined by microscopic examination of the blast cells. Blast cells from bone marrow samples are dyed and then examined via light microscopy. ALL cells are further categorized into three groups; L1, L2 and L3 cells. L1 cells, which represent the most common ALL morphology, are small, uniform blast cells that have round nuclei and scant cytoplasm. L2 cells have irregularly shaped nuclei, and size and amount of cytoplasm vary. L3 cells resemble Burkitt's lymphoma cells, and are uncommon. AML cells are categorized into 7 groups by FAB classification, M1 through M7. M1 cells are undifferentiated myeloblastic cells, M2 are differentiated (mature) myeloblastic cells, M3 are promyelocytic cells, M4 are myelomonoblastic cells, M5 are monoblastic cells, M6 are erythroleukemic cells and M7 are megakaryoblastic cells. The clinical importance of the FAB classification system has been shown in many studies (Lilleyman, 1986). Although this system is subjective and is used in combination with other diagnostic tests, it is a very important prognostic tool.

This study focuses on the use of confocal microscopy to develop a new method of identifying the particular type of leukemia a patient has, based on cell morphology features. In a

similar way to the FAB system, cells examined in this study were described by their cell morphology, size, nuclear morphology and mitochondrial distribution. Unlike the cell images seen under a conventional light microscope, the confocal z-stack image collections for each cell allow the ability to attain additional information along the third dimension perpendicular to the image plane. For instance, instead of just seeing an irregularly shaped nucleus in one plane, you can visualize where the indentations or lobes are that cause the nucleus to be irregular.

**Treatment.** The purpose of most leukemia treatments is to reduce the number of cancerous cells in the bone marrow so that normal blood cells can resume development. Typical treatments include chemotherapy, radiation therapy, and stem cell or bone marrow transplantation. Chemotherapy is the use of chemical agents to kill cancerous cells, and is considered a systematic treatment. Radiation therapy is the use of ionizing radiation to kill cancerous cells in a target area or tissue. Stem cell and bone marrow transplants are used to replenish normal blood cells when they have been severely depleted by leukemia. Immunotherapy is a relatively new type of treatment that uses the body's own immune system to eliminate cancerous cells. Surgery, chemotherapy, and radiotherapy are effective for reducing tumor burden, and immunotherapy might effectively be used to attack residual tumor cells to reduce the risk of recurrent disease and metastasis, and prolong patient survival (Gao 2007). Immunotherapy uses biological response modifiers (BRMs), including monoclonal antibodies and interferons, to help restore the immune system's ability to fight off cancer, and also lessens the side effects of some other treatments. The aim of antibody-mediated immunotherapy is to achieve specific binding of an antibody to leukemic cells, followed by clearance of the leukemic cells via antibody-dependent cell cytotoxicity (ADCC) or complement activation (Smits 2009).

Other drugs that target specific proteins found in certain types of leukemia cells are also

under development. Gleevec, a tyrosine kinase inhibitor, is one example that is already FDA approved and in use to treat Philadelphia chromosome positive chronic myeloid leukemia (Ph<sup>+</sup> CML). It targets and turns off specific proteins in the leukemic cells that allow them to develop. Gleevec has largely replaced allogeneic hematopoietic cell transplantation (HCT) as the first line therapy for chronic myeloid leukemia (Lee 2008). Nearly all patients attain hematologic remission, and 75% achieve cytogenetic remission (Kim 2008). Development of these target specific types of treatments is a new and promising area of leukemia research.

**Leukemic Cell Lines.** The establishment of leukemic cell lines has proved to be an invaluable tool in the area of leukemia research. Immortal cell lines provide an inexhaustible source of identical, malignant cells free of contamination (Chervinsky 2001). Important advantages of these cells are their unlimited supply, worldwide availability, monoclonal origin and ease of manipulation. Leukemic cell lines are ideally clones derived from a single cancerous cell, so the cell lines therefore consist of cells carrying the mutation that originally caused the cancer. The first malignant hematopoietic cell lines, which were Burkitt's lymphoma derived, were established in 1963; since then, numerous cell lines have been described (Drexler 2005). However, new leukemic cell lines are often difficult to establish, with most attempts failing for unknown causes. The reason for frequent failure of establishing new cell lines is unclear, although the major causes appear to be culture deterioration with a decrease in viability and overgrowth by normal cells in the culture (Drexler 2005). Another problem with malignant cell lines is the possibility that cells which become immortalized were selected for their ability to grow in-vitro, and the cell line might not be truly representative of the primary malignancy (Chervinsky 2001). Nevertheless, leukemic cell lines have proven to be irreplaceable in the

study of leukemia, and will continue to play a crucial role with the emergence of new anticancer therapies.

### **Confocal Microscopy**

**Overview.** Confocal laser scanning microscopy is an optical imaging technique that is capable of reconstructing three-dimensional images of specimens. A confocal microscope uses two principal ideas: point by point illumination of the sample and rejection of out of focus light (Prasad 2007). Unlike a conventional microscope that floods the whole specimen with light, confocal microscopy uses point illumination. This is achieved by directing a laser beam through a pinhole onto the sample, which reflects a light signal at the same wavelength or excites a fluorescent light signal at a different wavelength, back through another pinhole before being detected. As a result, out-of-focus signal is eliminated before it reaches the detector and a higher quality two-dimensional image is attained, once the focusing point is scanned within the focal plane. This is followed by translating the cell sample along the optical axis, or the z-axis, of the microscope objective and repeating the scanning again for another 2D image. This sequence of 2D imaging and sample translation along the z-axis at a preset step size is eventually used to produce a set of so-called z-stack images, which can be used to reconstruct the 3D structure of the cell sample (Brock 2006). The utility of confocal microscopy relies on its fundamental capacity to reject out-of-focus light, thus providing sharp, high-contrast 2D images of cells of very short focal depth and 3D subcellular structures within a thick sample (Dailey 1999). The majority of confocal microscopes image by stimulating fluorescence from dyes applied to the specimen (Semwogerere 2005). A series of lasers can be used to excite specimens that have been labeled with different fluorescent dyes. The availability of a variety of excitation wavelengths on a single microscope setup offers the power and convenience of using

combinations of fluorescent probes in a single specimen (Dailey 1999). This allows users to stain different parts of a cell, so that they show up differentially when imaged. In this study for instance, the nuclei and mitochondria of leukemia cells will be stained with different dyes, allowing us to detect them separately when imaging. Differences in the cells morphology can therefore be visualized.

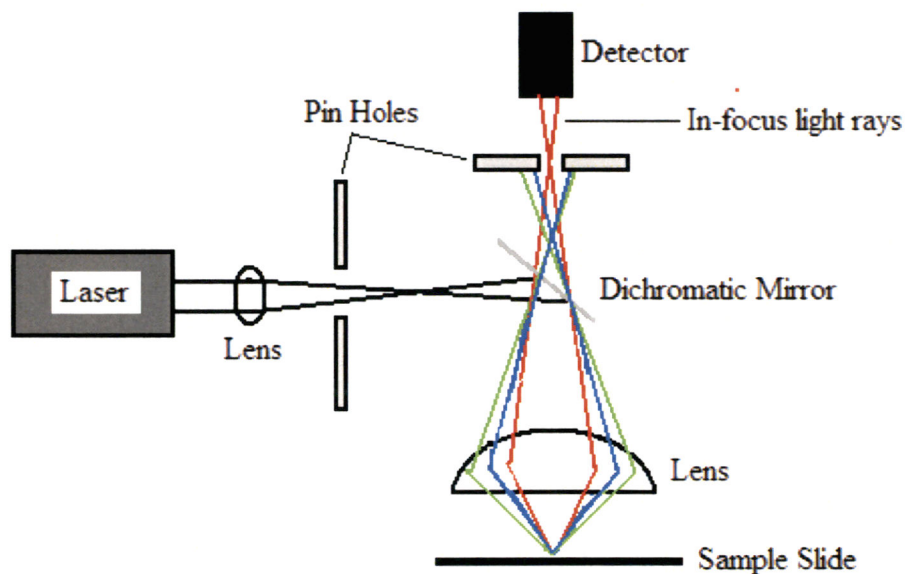


**Figure 1:** Schematic of a confocal laser scanning microscope. Out of focus light is blocked by pin-holes, helping create sharp, high-contrast two-dimensional images.

**Confocal imaging.** In recent studies, confocal imaging has been used to examine a variety of cancer related topics, from apoptosis and anti-cancer drug effectiveness to *in-vivo* diagnostics. An example would be testing the effectiveness of Harringtonine, an anti-cancer drug that is capable of inducing apoptosis in the acute myeloid leukemia HL-60 cell line. Confocal microscopy and two-photon laser scanning microscopy were used to simultaneously observe the nuclear morphology, mitochondrial potential and intracellular calcium concentration

of Harringtonine treated HL-60 cells (Zhang 2001). In another study, decreased mitochondrial integrity in UV exposed Jurkat cells was detected by confocal microscopy, indicative of apoptosis (Peters 2002). One of the most promising applications of confocal microscopy is its potential ability to diagnose many types of cancer *in-vivo*. Skin, esophageal, cervical and gastrointestinal are some of the types of cancer that have been examined by confocal microscopy. A laser scanning confocal endoscope has been developed that can generate high-quality images of both living cancer cells and normal cells in the gastrointestinal tract, with a quality comparable to that possible with conventional cytology (Inoue 2005). There have been multiple studies where confocal microscopy was combined with Raman spectroscopy for *in-vivo* analysis of human skin. The use of Raman spectroscopy for *in-vivo* skin research can be improved upon by combining it with confocal laser scanning microscopy, which allows more precise targeting of a skin structure for the Raman measurements (Arrasmith 2008). *In vivo* confocal microscopy enables real-time imaging of living tissue at high resolution and high contrast without physically dissecting the tissue, and confocal images can show cellular and nuclear structure in the epidermis, collagen fibers in the dermis, and circulating blood cells in dermal capillaries, as well as structures such as sebaceous glands, hair and hair follicles, and sweat ducts (Caspers 2003). Optical microscopic techniques, including *in-vivo* confocal laser scanning microscopy, offer unique possibilities for noninvasive skin research and skin characterization at high spatial resolution (Caspers 2003).

### **Experimental Cell Lines**

**NALM-6.** The NALM-6 cell line is an immortalized line of human pre-B leukemic cells. The cell line was originally established in 1976 from the peripheral blood of a 19-year-old male in his first relapse of acute lymphoblastic leukemia (ALL). Blood cultures from this patient led to the establishment of eight leukemic cell lines, Null Acute Leukemia-

Minowada (NALM) 6-13, and two “normal” B-cell lines, B85 and 86 (Minowada 1978). The NALM-6 line was characterized by Hurwitz et al in 1979 as medium to large lymphoid cells with a large nuclear to cytoplasmic ratio. The cytoplasm was limited to a narrow ring around a large, indented nucleus, and nucleoli were not prominent (Hurwitz 1979). They grow as single cells in suspension, with no adherence to the culture flask. NALM-6 cells are used extensively to study ALL, B-cell differentiation, apoptosis, and anticancer treatments.

**Jurkat.** The Jurkat cell line, originally named JM, is an immortalized line of human mature leukemic T lymphocyte cells. It was established from the peripheral blood of a 14 year old boy with T-cell leukemia during the first relapse of the disease. The cell line grows as single cells in suspension, with no adherence to the culture flask, no cytoplasmic projections and no colony formation. They have a smooth cell membrane, sparse cytoplasm, dentate nucleus, marginal chromatin distribution, prominent nucleolus, underdeveloped endoplasmic reticulum, well developed Golgi apparatus, and swollen mitochondria are frequently detected (Schneider 1977). Jurkat cells are often used to study types of T-cell leukemia.

**U937.** The immortalized human U937 cell line is a leukemic monocyte lymphoma cell line that is used as an in vitro model for studying monocyte/macrophage differentiation. It was established in 1976 from a patient with a diffuse histiocytic lymphoma. U937 cells are mostly round in shape, some with cytoplasmic projections, and a mean cell diameter 12.5 $\mu$  (Sundstrom 1976). They contain a moderate amount of granular cytoplasm, with few vacuoles. Nuclear shape is variable, with indentations and lobation regularly seen, often containing 1-2 nucleoli. During characterization, transmission electron microscopy was used to show the highly lobated nuclei (Sundstrom 1976). U937 cells grow as a single-cell suspension with no tendency to aggregate or adhere.

**HL-60.** The HL-60 cell line was established in 1977 from the peripheral blood of an adult female patient with acute promyelocytic leukemia. The cells largely resemble promyelocytes but can be induced to differentiate in vitro, and exhibit other features that make them an attractive model for studies of human myeloid cell differentiation (Birnie 1988). These AML cells grow as single cells suspension with no adherence or clumping. They are typically round to ovoid in shape, with a large round nucleus, and basophilic granular cytoplasm (Gallagher 1979). The majority of cells exhibit a myeloblastic/promyelocytic morphology as described above, with some cells of a more mature morphology, such as myelocytes, neutrophils and monocytes. The HL-60 cell line provides a continuous source of human cells for studying the events of myeloid differentiation (Gallagher 1979).

## MATERIALS AND METHODS

### Cell Lines

A representative acute lymphoid leukemia (ALL) cell line for both the B lymphocyte and T lymphocyte cell types were chosen to be the focus of this study. The Nalm-6 cell line was selected as the B lymphocyte line, as they are a human pre-B leukemia cells. The Jurkat cell line, an ALL human mature leukemic cell line, was selected to represent T lymphocytes. Two other acute myeloid leukemia (AML) cells lines were also imaged for comparison, which were the HL-60 human promyelocytic leukemia cell line, and the U937 human monocytic lymphoma cell line.

Each of the four cell lines were kept suspended in 10 ml of the appropriate culture media and were incubated at 35°C with 5% CO<sub>2</sub>. The Nalm-6 cells were grown in Minimum Essential Medium (MEM) with 10% FBS, while the Jurkat, HL-60 and U937 cell lines were cultured in RPMI media with 10% FBS. The cell lines were kept at a concentration of approximately 2x10<sup>6</sup> cells/ml, and each was split by a 1:10 dilution in the appropriate media 1-2 times every 5-7 days, as needed. Periodic cell counts were performed by staining the cells with trypan blue and using a hemocytometer and light microscope.

### Cell Preparation from blood samples

Human peripheral whole blood samples were obtained from two healthy, non-leukemic volunteers on separate occasions. Upon withdrawal, the blood sample was separated into two flasks. Each flask was treated with one of two mitogens to stimulate cell differentiation. The first flask was treated with Lectin from *Phaseolus vulgaris*, a type of phytohemagglutinin (PHA), for a period of 72 hours, which stimulated blood lymphocytes to develop into T-cells. The second flask received a phorbol ester, 12-0-tetradecanoyl-phorbol-13-acetate (TPA), which

stimulated B-cell differentiation. Since this study focuses specifically on the blood lymphocytes, they were first separated from the whole blood sample. This was achieved by gradient centrifugation. Five ml of the whole blood sample was carefully layered onto 3ml of LymphoSep lymphocyte separation medium in a 15ml centrifuge tube. The sample was then centrifuged at 400 g for 20 minutes. This process isolates the lymphocytes which can then be taken out and prepared for confocal imaging.

A human bone marrow or peripheral whole blood sample was also taken from six different leukemia patients, courtesy of Dr. Lilian Burke of the Brody School of Medicine at East Carolina University. See Table 1 below for details of each cell type used in this study, including each of the patient samples. Of the six patient samples, there were three AML samples, two ALL samples, and one sample that was undiagnosed. The bone marrow or peripheral blood was drawn from each patient by a staff member at the Leo W. Jenkins Cancer Center, part of the Brody School of Medicine. The samples were heparinized to prevent clotting, and were refrigerated until the time of use. These samples were not stimulated in any way. The leukocytes were separated out of each sample via the same LymphoSep gradient centrifugation protocol mentioned above, or similar Ficoll-Paque gradient, and were then prepared for imaging.

**Table 1: Cell Information Table**

Sample Name	Sample Type	Leukemia Type	Notes
Nalm-6	Cell Line	ALL	Cells cultured to approximately $3.0 \times 10^6$ cells/mL in MEM
Jurkat	Cell Line	ALL	Cells cultured to approximately $3.0 \times 10^6$ cells/mL in RPMI
HL-60	Cell Line	AML	Cells cultured to approximately $3.0 \times 10^6$ cells/mL in RPMI
U937	Cell Line	AML	Cells cultured to approximately $3.0 \times 10^6$ cells/mL in RPMI
PHA Stimulated	Peripheral Blood	Non-leukemic	Cells imaged approximately 72 hours after sample taken
TPA Stimulated	Peripheral Blood	Non-leukemic	Cells imaged approximately 72 hours after sample taken
Patient # 1	Bone Marrow	ALL	Cells imaged approximately 24 hours after sample taken
Patient # 2	Bone Marrow	AML	Cells imaged approximately 24 hours after sample taken
Patient # 3	Peripheral Blood	Undiagnosed	Cells imaged approximately 24 hours after sample taken
Patient # 4	Bone Marrow	AML	Cells imaged approximately 24 hours after sample taken
Patient # 5	Bone Marrow	AML	Cells imaged same day as sample taken
Patient # 6	Peripheral Blood	ALL	Cells imaged approximately 24 hours after sample taken

### Cell Staining

Each of the cell lines and blood cell sets mentioned above were stained with two fluorescent dyes prior to imaging with the confocal microscope. The dyes used were Mitotracker-Orange, a mitochondrial dye, and Syto-61, a nuclear dye, all purchased from Invitrogen. Mitotracker-Orange is a cell-permeant stain that passively diffuses across the plasma membrane and accumulates inside active mitochondria. Syto-61 is a cell-permeant red fluorescent stain that is activated upon binding with nucleic acids. These fluorescent dyes are excited by the lasers of the confocal microscope, allowing the mitochondria and nuclei of the cells to be visible during the imaging process. Syto-61 was used at a concentration of  $1 \mu\text{M}$ , while the Mitotracker-Orange was used at a concentration of  $200 \text{ nM}$ . One  $\mu\text{l}$  of each dye was added to 5 ml of cells in culture media. After an incubation time of 30 minutes, the cells were transferred to a centrifuge tube, pelleted by centrifugation, and resuspended in fresh culture media. The cells are then pelleted and resuspended in media a second time to wash away any

residual dye. A 150  $\mu$ l aliquot of the stained cells to be viewed were then placed on a depression slide and covered with a glass cover slip.

### **Confocal imaging**

Once the cells had been stained and prepared for viewing, they were imaged using a Zeiss LSM-510 confocal laser scanning microscope. The confocal microscope is located in the Flow Cytometry Facility at East Carolina University's Brody School of Medicine, under the direction of Dr. D. Weidner. Using the confocal microscope imaging software, the 633nm and 543nm lasers were selected and turned on for excitation of the nuclear and mitochondrial dyes. The LP 650 and BP 560-615 wavelength filters were used during fluorescence imaging. The long pass filter allows wavelengths longer than 650nm to pass through, while the bandpass filter allows wavelengths between 560 and 615nm to pass. A 100-150  $\mu$ l aliquot of the stained cells were placed on a glass depression slide and covered with a cover slip. The slide was placed under the 63x water immersion objective lens (Zeiss PN 440668) of the confocal microscope, and a drop of water was added before sliding the objective lens into place. A fluorescent backlight was used to visualize the cells through the binocular eyepiece of the confocal microscope, and a single cell was randomly chosen for imaging from the sample on the slide. The imaging software was used to zoom in on the cell for positioning of the objective, and then identify the first and last slides for the z-scan through the cell volume. A full collection of z-stack image stacks were then taken of the cell. There were around 40 images collected for each cell type, with one stack for each randomly selected cell.

### **Comparison of cell images**

This study was specifically looking for differences in cellular morphology between the cell types that were imaged. It has been shown that leukemic mitochondria have differences in

area per cell well as structural differences when compared with “normal” mitochondria (Schumacher 1975). Since the nuclei and mitochondria were stained prior to imaging, any differences within these organelles would be expected to be visible. The z-stack images for each cell were observed to determine overall cell morphology, cell size, nuclear morphology, and mitochondrial distribution.

**Table 2: Morphological Definitions**

Round	Appears circular throughout the z-stack images, consistent with an overall round object shape.
Oval	Has z-stack slices that typically begin round, leading to oval shaped images toward the center slice of the cell image stack. Some images appear ovoid throughout.
Elongated	Appear as a long, exaggerated oval shape.
Irregular	Appears to have no defined shape throughout the image stack.
Kidney	Presents kidney-shaped images towards the center slice of the image stack. Usually begins and ends with ovoid images at the edges of the nucleus.
Lobed	Contain lobed or globular extensions that protrude from the center of the cell/nucleus.
Clustered	Any set of mitochondria that are tightly grouped together in one area of the cell.
Granular	Showing granulated, textured structure.

For the overall cell morphology, the collective z-stack images for each cell were examined, slice by slice, to determine the shape of the cell. Based on the two-dimensional image slices, each cell was categorized as round, oval, elongated, or irregular, as shown by examples in Figure 2.

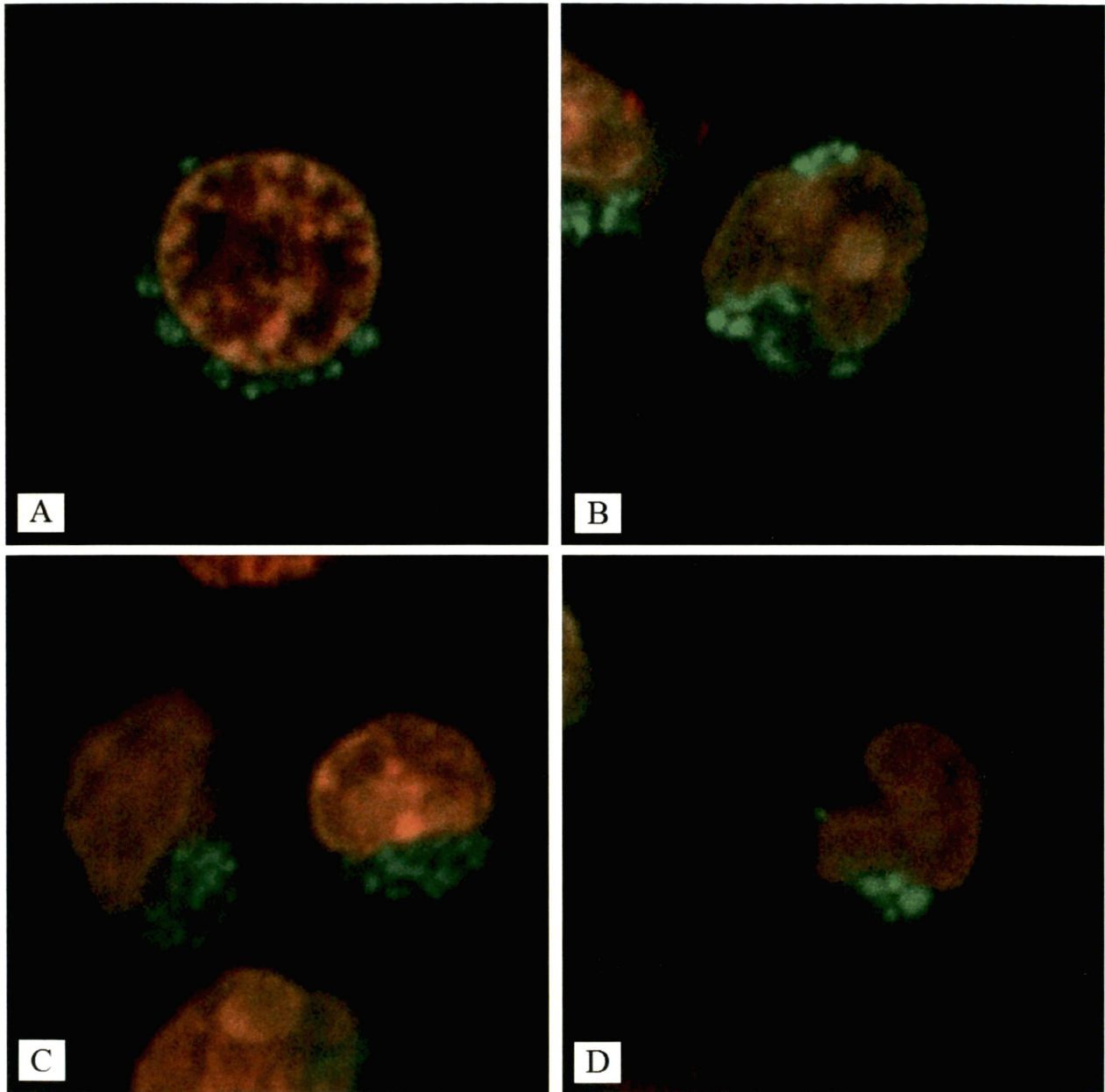


**Figure 2: Overall Cell Morphology** A. HL-60 image #39 - Round- Appears circular throughout the z-stack images, consistent with an overall round shape. B. Nalm-6 image #14 - Oval - Has z-stack slices that typically begin round, leading into oval shaped cell images near the center of the cell. Some with ovoid shaped cell images throughout z-stack. C. PHA cell #12 - Elongated - Cell images show an elongated oval-shaped cell. D. Nalm-6 image #16 - Irregular - Any set of z-stack images where the cell appears to have no defined shape. Some images appear globular or lobed.

To determine cell size, the built in micrometer scale of the Zeiss LSM Image Browser software was used to measure the overall diameter of each cell. The z-stack slice that best represented the centermost portion of the cell was chosen to make the measurement, and only the round cells could be measured to attain an accurate diameter. Margins were set on the edges of the cell membrane, and the integrated scale was used to calculate the cell size down to 0.5 $\mu\text{m}$ . The diameter recorded for each cell represents a 2-dimensional measurement.

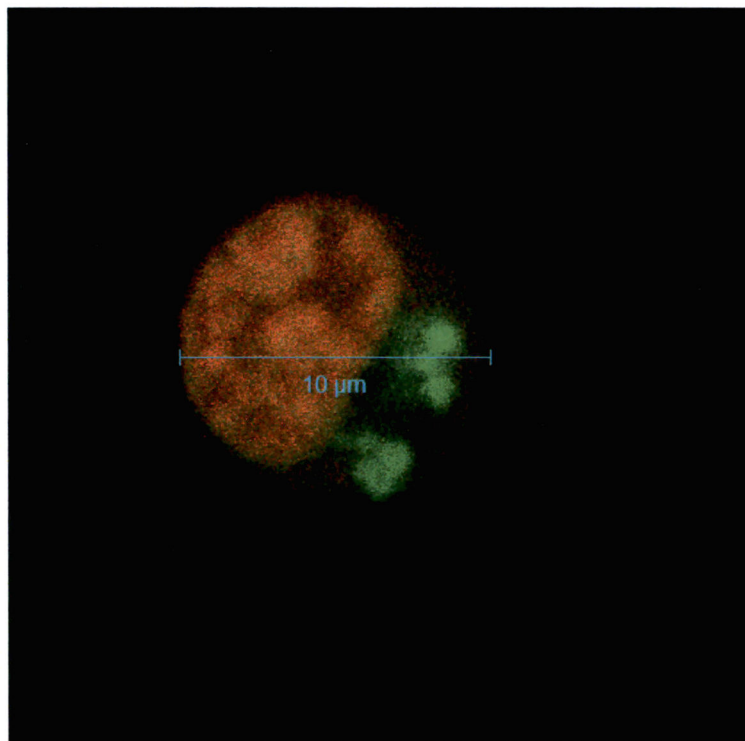


**Figure 3:** Jurkat image #28, measured at 10 $\mu\text{m}$  across the diameter.

Since the cell lines were each stained with the Syto-61 nuclear dye, the LSM Image Browser software picked up the fluorescence from the dye and presented it as a red color on the cell images, making the nucleus for each cell readily discernable. Like the overall cell morphology, the nuclear morphology was determined by observing the z-stack collection for

each cell, slice by slice. Each nucleus was classified as having a round, oval, kidney, or irregular shape, in a very similar manner as described for the overall cell morphology. Some irregular shaped nuclei were further categorized as being lobed and/or elongated. Notations were also made for each cell describing the granularity of the nucleus.

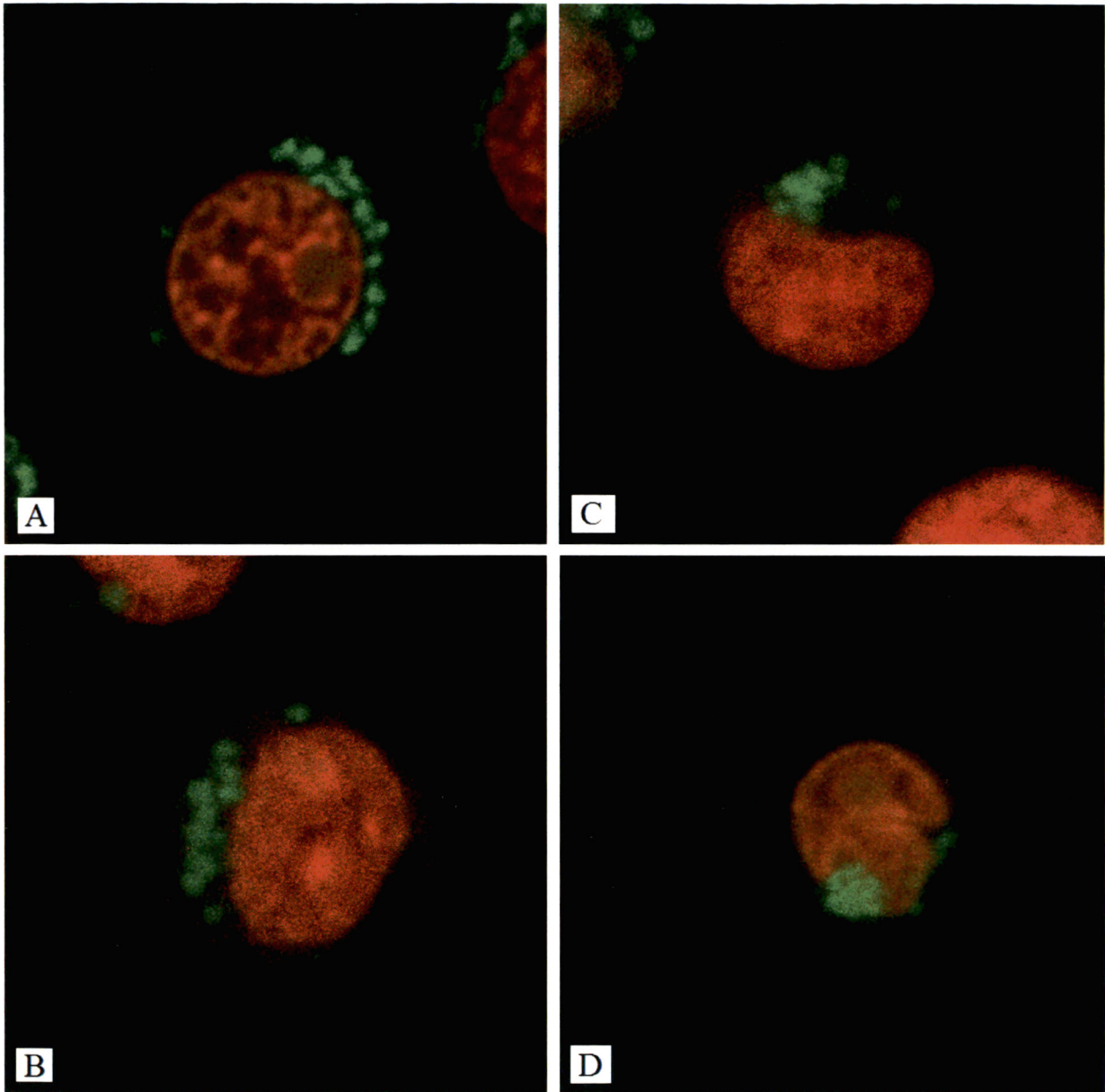


**Figure 4: Nuclear Morphology** A. HL-60 image #28 - Round- Nucleus appears circular throughout the z-stack images. B. U937 image #7 - Oval - Has z-stack slices that typically begin round, leading into oval shaped cell images near the center of the cell. Some with ovoid shaped cell images throughout z-stack. C. Jurkat image #24 - Kidney - Cell images show kidney shaped nucleus near the center of the cell. D. Nalm-6 image #34 - Irregular - Any set of z-stack images where the cell appears to have no defined shape. Some images appear globular or lobed.

The image software displayed the Mitotracker-Orange mitochondrial dye using a green color to represent the reflected fluorescence. To categorize the cells based on mitochondrial distribution, the z-stack for each cell was observed slice by slice to decide how the mitochondria were dispersed throughout the cell. A brief description was given for each cell, noting whether or not the mitochondria were clustered together or evenly spread inside the cell. If the mitochondria were deemed clustered, the area of the cell where the cluster was located in relation to the nucleus was also noted. Quantification of mitochondria in each cell was not possible due to poor clarity of individual mitochondria, as clusters of mitochondria often blended together.

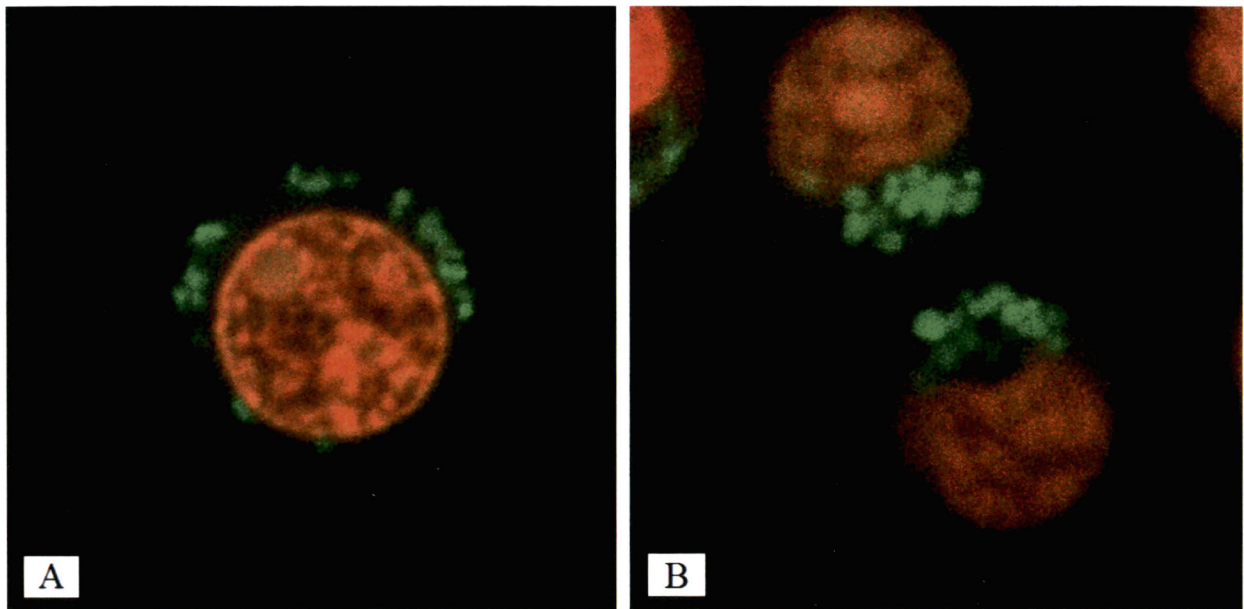


**Figure 5: Mitochondrial Distribution** A. HL-60 image #32 – Mitochondria dispersed around the nucleus. B. Jurkat image #22 – Mitochondria clustered together in one area beside the nuclei.

## **RESULTS**

### **Cell Imaging**

A field-of-view containing multiple cells was visually chosen under the eyepiece of the confocal microscope. A particular field-of-view was selected based on how well the cells inside it were able to absorb the nuclear and mitochondrial dyes during incubation. Any cells that did not absorb the dyes, absorbed them unevenly, or exhibited too strong a fluorescence were avoided. The selected field-of-view was then scanned with the focused beam to attain a single confocal image slice of the multiple cells within it. A single cell was randomly selected from this confocal image to capture a z-stack image. The Zeiss imaging software was used to zoom in on that single cell, and to set the points above and below the cell for which the sample glass slide would be translated along the z-axis to attain the image stack. The cell image would be named and saved on the computer's hard drive.

### **Comparing Cell Images**

Each slice of the z-stack cell images was examined and morphological features were recorded into a spreadsheet according to the definitions given in Table 2 and Figure 2. The features of interest included overall cell morphology, cell size, nuclear morphology, and mitochondrial distribution throughout the cell. Once all of the cells for a cell line or blood sample had been examined, the images for that particular cell line were compared to each other. The cell sizes were all averaged, and an overall morphology was determined for each cell line and blood sample. Due to the clonality of the four cell lines, the results for each was very uniform. Within each of the blood samples however, there was considerably more variance. This could be due to contamination of the samples with other cell types, or the cells being in different stages of cell cycle. Once the data for all of the samples was compiled, the cell lines

and blood samples were compared to each other.

### **Nalm-6 Cell Line**

The human Nalm-6 pre-B ALL cells were the first to be imaged. They are round cells, with an average  $9.73\mu\text{m}$  cell diameter. The nuclei of these cells are irregularly shaped, with lobed protrusions. The mitochondria are together in clusters, where in about half the cells they are concentrated in one location beside the nucleus, with the other half having them clustered all around the nucleus.

### **Jurkat Cell Line**

The Jurkat cell line was the second ALL cell in used in this study. These human mature leukemic T-cells are round in shape, with an average diameter of  $9.5\mu\text{m}$ . The nuclei in these cells had a granular appearance, and were typically round to oval in shape, with a very few cells exhibiting kidney shaped nuclei. The mitochondrial distribution was very uniform in all the Jurkat cells imaged. They were all clustered together beside the nucleus of each cell, typically in one spot.

### **HL-60 Cell Line**

The HL-60 cell line, which are human promyelocytic leukemia cells, are larger than both the Nalm-6 and Jurkat cell lines mentioned above. These AML cells are also round in shape, but have an average  $11.36\mu\text{m}$  cell diameter. The nuclei of the cells that were imaged are almost all round in shape, with a granular appearance. The mitochondria of these HL-60 cells were also uniform, being clustered together all around the nucleus.

### **U937 Cell Line**

Like the HL-60 cell line, the U937 human leukemic monocyte lymphoma cells are also larger than both ALL cell lines, at an average  $11.79\mu\text{m}$  cell diameter. These cells are round, with

typically granular, irregularly shaped nuclei. Some of these irregular shaped nuclei have protruding lobes, while a few of the U937 cells have nuclei with a more basic oval shape. Most cells have the mitochondria clustered together beside or surrounding the nuclei.

### **TPA Stimulated Cells**

The TPA stimulated human B-cells had an overall round to oval shape, with an average cell diameter of  $9.82\mu\text{m}$ . The nuclear morphology varied between irregular with lobes and round shaped nuclei, and the mitochondria were clustered together on the sides of the nucleus.

### **PHA Stimulated Cells**

The PHA stimulated human T-cells also had an overall round to oval shape, with a  $10.53\mu\text{m}$  average cell diameter. Two of the cells imaged were elongated, with a  $14\text{-}15\mu\text{m}$  overall length. The nuclei were granular, and varied from a round-oval shape to an irregular shape. The mitochondria were mainly clustered beside the nucleus of each cell.

### **ALL Patient Cells**

The ALL cells from Patient #1 had a round to ovoid overall shape, with an average cell diameter of  $8.54\mu\text{m}$ . There were several indented (kidney shaped) nuclei, but the majority were irregularly shaped and granular, and the mitochondria tended to cluster in one area beside the nucleus.

The ALL cells from Patient #6 had a round overall shape, with an average cell diameter of  $8.63\mu\text{m}$ . The nuclei were granular, irregular in shape, and most were lobated. The mitochondria in each cell were clustered together in one area beside the nucleus.

### **AML Patient Cells**

The AML cells from Patient #2 were mostly round in shape, with a few round cells. The average cell diameter of the measurable round cells was  $9.33\mu\text{m}$ . The nuclei were granular and mostly irregularly shaped, many of which were lobated, and few kidney shaped nuclei were observed. The mitochondria were typically grouped together in one area beside the nuclei.

Cells from Patient #4 had an average cell diameter of  $9.17\mu\text{m}$ , with an overall round to ovoid cell shape. The nuclei were granular, and shape varied between round and irregular. Mitochondria were clustered throughout the cytoplasm around the nuclei.

The overall shape of the AML cells from Patient #5 varied greatly. The average cell diameter of the measurable round cells was  $9.88\mu\text{m}$ . Nuclei were granular and irregularly shaped, most with lobed protrusions. Mitochondrial distribution also varied, with most cells having them clustered in 1-2 areas, and some having them dispersed throughout the cytoplasm.

### **Undiagnosed Patient Cells**

The cells isolated from patient #3 were round to ovoid in shape, with a largely varying cell diameter. The average cell diameter was  $8.19\mu\text{m}$ , with a range of  $6\text{-}12\mu\text{m}$  in size. The nuclei were round and granular, with the mitochondria clustered together around the nucleus or in areas beside the nucleus.

**Table 3:** Results taken from NALM-6 confocal images.

<b>Nalm-6 Cells:</b> Human Pre-B ALL Cell Line				
<b>Image</b>	<b>Cell Morphology</b>	<b>Cell Diameter (µm)</b>	<b>Nuclear Morphology</b>	<b>Mitochondrial Morphology</b>
1	Round	10.5	Irregular, lobed, granular	Clustered above and beside nucleus
2	Oval	na	Irregular, lobed, granular	Clustered beside nucleus
3	Round	10.5	Round, granular	Clustered beside and below nucleus
4	Round	11	Irregular, lobed, granular	Clustered above and beside nucleus
5	Round	10.5	Irregular, lobed, granular	Clustered beside and below nucleus
6	Oval	na	Irregular, lobed, granular	Clustered beside nucleus
7	Round	10	Irregular, lobed, granular	Clustered around nucleus
8	Irregular	na	Irregular, lobed, granular	Clustered around nucleus
9	Round	11.5	Irregular, lobed, granular	Clustered around nucleus
10	Round	10	Irregular, lobed, granular	Clustered around nucleus
11	Irregular	na	Irregular, lobed, granular	Clustered beside and below nucleus
12	Round	10.5	Irregular, lobed, granular	Clustered beside and below nucleus
13	Round	11.5	Irregular, lobed, granular	Clustered beside and below nucleus
14	Oval	na	Irregular, lobed, granular	Clustered around nucleus
15	Oval	na	Irregular, lobed, granular	Clustered beside nucleus
16	Irregular	na	Irregular, lobed, granular	Clustered beside nucleus
17	Round	9	Irregular, lobed, granular	Clustered around nucleus
18	Round	10.5	Irregular, lobed, granular	Clustered beside nucleus
19	Round	8	Irregular, lobed, granular	Clustered beside nucleus
20	Round	8.5	Irregular, lobed, granular	Clustered beside and below nucleus
21	Round	10	Irregular, lobed, granular	Clustered beside nucleus
22	Round	10	Irregular, lobed, granular	Clustered beside nucleus
23	Round	10	Irregular, lobed, granular	Clustered around nucleus
24	Round	10	Irregular, lobed, granular	Clustered beside and below nucleus
25	Round	10.5	Irregular, lobed, granular	Clustered around nucleus
26	Round	9	Irregular, lobed, granular	Clustered around nucleus
27	Round	10	Irregular, lobed, granular	Clustered beside nucleus
28	Round	10	Irregular, lobed, granular	Clustered around nucleus
29	Round	10.5	Irregular, lobed, granular	Clustered above and below nucleus
30	Round	11	Irregular, lobed, granular	Clustered beside and below nucleus
31	Oval	na	Irregular, lobed, granular	Clustered above and beside nucleus
32	Round	8.5	Irregular, lobed, granular	Clustered around nucleus
33	Round	8	Irregular, lobed, granular	Clustered beside and below nucleus
34	Round	8.5	Irregular, lobed, granular	Clustered beside nucleus
35	Round	9	Irregular, lobed, granular	Clustered around nucleus
36	Oval	na	Irregular, lobed, granular	Clustered above and below nucleus
37	Round	8	Irregular, lobed, granular	Clustered beside nucleus
38	Round	9	Irregular, lobed, granular	Clustered beside nucleus
39	Round	9	Irregular, lobed, granular	Clustered beside nucleus
40	Round	8.5	Round, granular	Clustered beside nucleus

**Table 4:** Results taken from Jurkat confocal images.

<b>Jurkat Cell Line:</b> Human mature leukemic T-cells				
<b>Image</b>	<b>Cell Morphology</b>	<b>Cell Diameter (µm)</b>	<b>Nuclear Morphology</b>	<b>Mitochondrial Morphology</b>
1	Round	8.5	Round, granular	Dispersed around nucleus, clustered
2	Round	9.5	Round, granular	Clustered beside nucleus
3	Round	10	Round, granular	Clustered beside nucleus
4	Round	8	Oval, granular	Clustered beside nucleus
5	Round	9	Oval, granular	Clustered beside nucleus
6	Round	9.5	Oval, granular	Clustered beside, below nucleus
7	Round	9	Kidney, granular	Clustered on each side of nucleus
8	Round	10	Oval, granular	Clustered beside nucleus
9	Round	11	Round, granular	Clustered beside nucleus
10	Round	9.5	Oval, granular	Clustered beside, below nucleus
11	Round	8	Oval, granular	Clustered beside nucleus
12	Round	9.5	Round, granular	Clustered beside nucleus
13	Round	8	Oval, granular	Clustered beside nucleus
14	Round	9	Round, granular	Clustered beside nucleus
15	Round	7.5	Round, granular	Clustered below nucleus
16	Round	8.5	Round, granular	Clustered beside nucleus
17	Round	8.5	Round, granular	Clustered beside, above nucleus
18	Round	9	Oval, granular	Clustered beside nucleus
19	Round	9	Round, granular	Clustered beside, above nucleus
20	Round	10.5	Oval, granular	Clustered beside nucleus
21	Round	9	Oval, granular	Clustered beside nucleus
22	Round	10	Kidney, granular	Clustered beside nucleus
23	Round	10	Oval, granular	Clustered beside nucleus
24	Round	10	Kidney, granular	Clustered beside nucleus
25	Round	10.5	Oval, granular	Clustered beside nucleus
26	Round	9	Round, granular	Clustered beside nucleus
27	Round	10	Kidney, granular	Clustered beside nucleus
28	Round	10	Oval, granular	Clustered beside nucleus
29	Round	10.5	Round, granular	Clustered beside nucleus
30	Round	11.5	Round, granular	Clustered beside nucleus
31	Round	10	Oval, granular	Clustered beside, above nucleus
32	Round	9	Oval, granular	Clustered beside nucleus
33	Round	9.5	Kidney, granular	Clustered beside nucleus
34	Round	9.5	Oval, granular	Clustered beside nucleus
35	Round	10	Oval, granular	Clustered beside, below nucleus
36	Round	10.5	Oval, granular	Clustered beside, above nucleus
37	Round	10	Oval, granular	Clustered beside nucleus
38	Round	10	Round, granular	Clustered beside, above nucleus
39	Round	11	Oval, granular	Clustered beside nucleus
40	Round	8.5	Oval, granular	Clustered beside nucleus

**Table 5:** Results taken from PHA stimulated non-leukemic T-cell confocal images.

<b>PHA Stimulated T-Cells</b>				
<b>Image</b>	<b>Cell Morphology</b>	<b>Cell Diameter (µm)</b>	<b>Nuclear Morphology</b>	<b>Mitochondrial Morphology</b>
1	Round	12.5	Irregular, granular	Clustered beside nucleus
2	Round	11	Round, granular	Clustered beside/below nucleus
3	Round	10	Oval, granular	Clustered beside/below nucleus
4	Round	10	Oval, granular	Clustered beside/below nucleus
5	Round	11	Round, granular	Clustered below nucleus
6	Round	10.5	Irregular, granular	Clustered beside nucleus
7	Round	10.5	Round, granular	Clustered beside nucleus
8	Elongated	NA	Irregular, elongated, granular	Clustered beside nucleus
9	Round	11	Irregular, granular	Clustered beside nucleus
10	Oval	NA	Irregular, lobed, granular	Clustered above/beside nucleus
11	Oval	NA	Round, granular	Clustered beside nucleus
12	Round	10	Oval, granular	Clustered beside nucleus
13	Oval	NA	Oval, granular	Clustered above/beside nucleus
14	Round	11	Oval, granular	Clustered beside nucleus
15	Round	10	Irregular, granular	Clustered beside nucleus
16	Elongated	NA	Irregular, lobed, granular	Clustered beside nucleus
17	Round	11	Round, granular	Clustered around nucleus
18	Round	10.5	Round, granular	Clustered beside/below nucleus
19	Round	11	Irregular, granular	Clustered around nucleus
20	Round	8	Round, granular	Clustered around nucleus

**Table 6:** Results taken from TPA stimulated non-leukemic B-cell confocal images.

<b>TPA Stimulated B-Cells</b>				
<b>Image</b>	<b>Cell Morphology</b>	<b>Cell Diameter (<math>\mu\text{m}</math>)</b>	<b>Nuclear Morphology</b>	<b>Mitochondrial Morphology</b>
1	Round	9.5	Irregular, lobed, granular	Clustered beside/below nucleus
2	Round	9	Irregular, lobed, granular	Clustered above/beside nucleus
3	Round	8.5	Irregular, granular	Clustered beside nucleus
4	Oval	NA	Irregular, granular	Clustered beside nucleus
5	Round	9	Irregular, lobed, granular	Clustered around nucleus
6	Round	8.5	Irregular, granular	Clustered beside nucleus
7	Round	9.5	Irregular, lobed, granular	Clustered above/beside nucleus
8	Round	8	Round, granular	Clustered below nucleus
9	Round	9	Irregular, lobed, granular	Clustered beside nucleus
10	Round	10.5	Irregular, granular	Clustered beside nucleus
11	Round	11	Irregular, lobed, granular	Clustered beside/below nucleus
12	Oval	NA	Round, granular	Clustered around nucleus
13	Round	10	Irregular, lobed, granular	Clustered beside nucleus
14	Round	9.5	Irregular, lobed, granular	Clustered around nucleus
15	Oval	NA	Round, granular	Clustered beside/below nucleus
16	Round	9.5	Irregular, granular	Clustered beside/below nucleus
17	Round	10	Round, granular	Clustered beside/below nucleus
18	Round	10.5	Irregular, granular	Clustered beside nucleus
19	Round	10	Oval, granular	Clustered around nucleus
20	Oval	NA	Round, granular	Clustered around nucleus
21	Round	10	Irregular, granular	Clustered above/beside nucleus
22	Round	7.5	Irregular, granular	Clustered beside nucleus
23	Round	10	Round, granular	Clustered around nucleus
24	Round	10	Round, granular	Clustered beside/below nucleus
25	Oval	NA	Round, granular	Clustered beside nucleus
26	Round	11	Round, granular	Clustered around nucleus
27	Round	10.5	Irregular, lobed, granular	Clustered below nucleus
28	Round	11	Irregular, granular	Clustered above/beside nucleus
29	Round	11.5	Irregular, lobed, granular	Clustered beside/below nucleus
30	Round	10	Round, granular	Clustered beside/below nucleus
31	Round	10	Round, granular	Clustered above/beside nucleus
32	Oval	NA	Irregular, lobed, granular	Clustered beside nucleus
33	Round	9	Irregular, granular	Clustered beside/below nucleus
34	Round	11	Oval, granular	Clustered beside nucleus
35	Round	11.5	Round, granular	Clustered above/beside nucleus
36	Round	9	Irregular, granular	Clustered beside nucleus
37	Round	10	Irregular, lobed, granular	Clustered beside nucleus
38	Round	11	Round, granular	Clustered beside nucleus
39	Oval	NA	Round, granular	Clustered beside nucleus
40	Round	9	Kidney, granular	Clustered beside nucleus

**Table 7:** Results taken from HL-60 confocal images.

<b>HL-60 Cells</b>				
<b>Image</b>	<b>Cell Morphology</b>	<b>Cell Diameter (μm)</b>	<b>Nuclear Morphology</b>	<b>Mitochondrial Morphology</b>
1	Round	10	Round, granular	Clustered around nucleus
2	Round	11	Round, granular	Clustered around nucleus
3	Round	12	Round, granular	Clustered around nucleus
4	Round	10.5	Round, granular	Clustered around nucleus
5	Oval	NA	Round, granular	Clustered around nucleus
6	Round	10.5	Round, granular	Clustered around nucleus
7	Round	12	Round, granular	Clustered around nucleus
8	Round	13	Round, granular	Clustered around nucleus
9	Round	11	Round, granular	Clustered around nucleus
10	Round	11	Round, granular	Clustered around nucleus
11	Round	12.5	Round, granular	Clustered around nucleus
12	Round	12	Irregular, granular	Clustered around nucleus
13	Round	12	Round, granular	Clustered around nucleus
14	Round	11	Round, granular	Clustered around nucleus
15	Round	10.5	Irregular, granular	Clustered around nucleus
16	Round	12	Kidney, granular	Clustered around nucleus
17	Round	11.5	Irregular, granular	Clustered beside/below nucleus
18	Round	12	Round, granular	Clustered around nucleus
19	Round	11	Round, granular	Clustered around nucleus
20	Round	11	Round, granular	Clustered around nucleus
21	Round	11	Round, granular	Clustered around nucleus
22	Round	12	Round, granular	Clustered around nucleus
23	Round	11	Round, granular	Clustered beside nucleus
24	Round	10	Round, granular	Clustered around nucleus
25	Round	12	Round, granular	Clustered around nucleus
26	Round	11	Round, granular	Clustered around nucleus
27	Round	11	Round, granular	Clustered beside/below nucleus
28	Round	12	Round, granular	Clustered around nucleus
29	Round	11.5	Round, granular	Clustered above/beside nucleus
30	Round	11.5	Round, granular	Clustered around nucleus
31	Round	10	Round, granular	Clustered around nucleus
32	Round	12	Round, granular	Clustered around nucleus
33	Oval	NA	Round, granular	Clustered around nucleus
34	Round	11.5	Round, granular	Clustered beside/below nucleus
35	Oval	NA	Round, granular	Clustered around nucleus
36	Oval	NA	Round, granular	Clustered above/beside nucleus
37	Round	11.5	Round, granular	Clustered above/beside nucleus
38	Round	12	Round, granular	Clustered around nucleus
39	Round	12.5	Round, granular	Clustered around nucleus
40	Round	10	Round, granular	Clustered above/beside nucleus

**Table 8:** Results taken from U937 confocal images.

<b>U937 Cells</b>				
<b>Image</b>	<b>Cell Morphology</b>	<b>Cell Diameter (µm)</b>	<b>Nuclear Morphology</b>	<b>Mitochondrial Morphology</b>
1	Round	12	Irregular, granular	Clustered on 2 sides of nucleus
2	Round	12	Irregular, lobed, granular	Clustered around nucleus
3	Round	11	Irregular, lobed, granular	Clustered around nucleus
4	Round	10.5	Irregular, lobed, granular	Clustered around nucleus
5	Round	11	Oval, granular	Clustered beside nucleus
6	Round	13.5	Irregular, lobed, granular	Clustered around nucleus
7	Round	13	Oval, granular	Clustered beside nucleus
8	Round	12.5	Irregular, granular	Clustered beside nucleus
9	Round	12.5	Oval, granular	Clustered around nucleus
10	Round	14.5	Irregular, granular	Clustered around nucleus
11	Round	11.5	Irregular, granular	Clustered around nucleus
12	Round	12	Oval, lobed, granular	Clustered beside nucleus
13	Round	12.5	Irregular, granular	Clustered beside nucleus
14	Round	11	Oval, granular	Clustered beside nucleus
15	Round	12.5	Irregular, granular	Clustered around nucleus
16	Round	12	Oval, granular	Clustered around nucleus
17	Round	12.5	Oval, granular	Clustered beside nucleus
18	Round	11.5	Irregular, lobed, granular	Clustered around nucleus
19	Round	12.5	Irregular, granular	Clustered beside nucleus
20	Round	11.5	Irregular, granular	Clustered around nucleus
21	Round	12	Irregular, lobed, granular	Clustered around nucleus
22	Round	11.5	Irregular, lobed, granular	Clustered around nucleus
23	Round	11	Irregular, lobed, granular	Clustered around nucleus
24	Round	11	Irregular, lobed, granular	Clustered beside nucleus
25	Round	11	Irregular, lobed, granular	Clustered beside nucleus
26	Round	11.5	Irregular, lobed, granular	Clustered around nucleus
27	Round	11.5	Irregular, granular	Clustered around nucleus
28	Round	11.5	Irregular, lobed, granular	Clustered around nucleus
29	Round	10	Irregular, lobed, granular	Clustered around nucleus
30	Round	12	Irregular, granular	Clustered around nucleus
31	Round	12	Irregular, granular	Clustered around nucleus
32	Round	10	Irregular, lobed, granular	Clustered around nucleus
33	Round	12.5	Kidney, granular	Clustered beside nucleus
34	Round	11.5	Irregular, lobed, granular	Clustered around nucleus
35	Round	10	Irregular, lobed, granular	Clustered around nucleus
36	Round	12.5	Oval, granular	Clustered around nucleus
37	Round	14	Irregular, lobed, granular, cell division	Clustered around nucleus
38	Round	11.5	Irregular, lobed, granular	Clustered around nucleus
39	Round	12	Irregular, lobed, granular	Clustered around nucleus
40	Round	10.5	Irregular, granular	Clustered around nucleus

**Table 9:** Results taken from Patient #1 (ALL) confocal images.

<b>Patient #1: ALL Cells</b>				
<b>Image</b>	<b>Cell Morphology</b>	<b>Cell Diameter (µm)</b>	<b>Nuclear Morphology</b>	<b>Mitochondria Morphology</b>
1	Round	8	Oval, granular	Clustered beside/below nucleus
2	Oval	NA	Round, granular	Clustered beside nucleus
3	Round	9	Irregular, lobed, granular	Clustered beside nucleus
4	Round	8.5	Irregular, lobed, granular	Clustered beside nucleus
5	Round	9	Irregular, granular	Clustered beside nucleus
6	Round	9	Kidney, granular	Clustered beside nucleus
7	Round	8.5	Kidney, granular	Clustered beside nucleus
8	Oval	NA	Irregular, granular	Clustered beside nucleus
9	Oval	NA	Irregular, granular	Clustered beside nucleus
10	Round	8	Irregular, granular	Clustered beside/below nucleus
11	Oval	NA	Irregular, lobed, granular	Clustered beside nucleus
12	Round	8	Irregular, lobed, granular	Clustered beside nucleus
13	Round	8	Oval, granular	Clustered beside nucleus
14	Round	8.5	Kidney, granular	Clustered beside nucleus
15	Oval	NA	Kidney, granular	Clustered beside nucleus
16	Irregular Round	NA	Irregular, granular	Clustered beside/below nucleus
17	Round	9.5	Irregular, granular	Clustered around nucleus
18	Irregular	NA	Irregular, lobed, granular	Clustered beside nucleus
19	Oval	NA	Irregular, lobed, granular	Clustered above/beside nucleus
20	Round	9	Irregular, lobed, granular	Clustered beside nucleus
21	Round	8	Kidney, granular	Clustered beside nucleus

**Table 10:** Results taken from Patient #2 (AML) confocal images.

<b>Patient #2: AML Cells</b>				
<b>Image</b>	<b>Cell Morphology</b>	<b>Cell Diameter (µm)</b>	<b>Nuclear Morphology</b>	<b>Mitochondria Morphology</b>
1	Oval	NA	Irregular, lobed, granular	Clustered beside/below nucleus
2	Oval	NA	Kidney, granular	Clustered beside nucleus
3	Oval	NA	Irregular, lobed, granular	Clustered beside nucleus
4	Oval	NA	Irregular, lobed, granular	Clustered beside/below nucleus
5	Oval	NA	Irregular, kidney, granular	Clustered beside nucleus
6	Oval	NA	Irregular, granular	Clustered beside/below nucleus
7	Round	10	Irregular, granular	Clustered beside nucleus
8	Round	8	Kidney, granular	Clustered beside nucleus
9	Oval	NA	Irregular, lobed, granular	Clustered beside/below nucleus
10	Oval	NA	Irregular, lobed, granular	Clustered beside nucleus
11	Round	9	Irregular, granular	Clustered beside nucleus
12	Oval	NA	Kidney, granular	Clustered beside nucleus
13	Oval	NA	Irregular, lobed, granular	Clustered beside nucleus
14	Round	9	Irregular, lobed, granular	Clustered beside nucleus
15	Oval	NA	Kidney, granular	Clustered beside nucleus
16	Round	10	Irregular, lobed, granular	Clustered beside/below nucleus
17	Oval	NA	Irregular, granular	Clustered beside/below nucleus
18	Oval	NA	Kidney, granular	Clustered beside nucleus
19	Oval	NA	Irregular, lobed, granular	Clustered beside nucleus
20	Irregular Round	~9	Irregular, granular	Clustered beside nucleus
21	Oval	NA	Kidney, granular	Clustered beside/below nucleus
22	Round	10	Irregular, granular	Clustered beside nucleus

**Table 11:** Results taken from Patient #3 (Undiagnosed) confocal images.

<b>Patient #3: Undiagnosed</b>				
<b>Image</b>	<b>Cell Morphology</b>	<b>Cell Diameter (µm)</b>	<b>Nuclear Morphology</b>	<b>Mitochondria Morphology</b>
1	Round	7	Round, granular	Clustered beside/below nucleus
2	Large Round	10.5	Round, granular	Clustered around the nucleus
3	Round	7	Round, granular	Clustered beside/below nucleus
4	Round	7	Round, granular	Clustered beside/below nucleus
5	Large Round	12	Round, granular	Clustered around the nucleus
6	Round	6	Round, granular	Clustered beside nucleus
7	Round	7.5	Oval, granular	Clustered beside nucleus
8	Oval	NA	Round, granular	Clustered beside/below nucleus
9	Round	7	Round, granular	Clustered beside/below nucleus
10	Oval	NA	Round, granular	Clustered beside/below nucleus
11	Round	6	Round, granular	Clustered below nucleus
12	Oval	NA	Round, granular	Clustered beside/below nucleus
13	Round	7	Round, granular	Clustered around the nucleus
14	Large Round	11	Round, granular	Clustered around the nucleus
15	Large Round	12	Round, granular	Clustered around the nucleus
16	Round	6.5	Round, granular	Clustered beside nucleus
17	Oval	NA	Round, granular	Clustered beside/below nucleus

**Table 12:** Results taken from Patient #4 (AML) confocal images.

<b>Patient #4: AML Cells</b>				
<b>Image</b>	<b>Cell Morphology</b>	<b>Cell Diameter (<math>\mu\text{m}</math>)</b>	<b>Nuclear Morphology</b>	<b>Mitochondria Morphology</b>
1	Round	8.5	Round, granular	Clustered around nucleus
2	Oval	NA	Irregular, granular	Clustered around nucleus
3	Oval	NA	Irregular, lobed, granular	Clustered around nucleus
4	Round	8	Irregular, granular	Clustered beside/below nucleus
5	Round	9	Irregular, granular	Clustered above/beside nucleus
6	Round	10.5	Irregular, granular	Clustered around nucleus
7	Round	9.5	Irregular, lobed, granular	Clustered around nucleus
8	Round	7.5	Irregular, granular	Clustered beside nucleus
9	Round	7.5	Round, granular	Clustered above/beside nucleus
10	Round	8	Round, granular	Clustered around nucleus
11	Oval	NA	Round, granular	Clustered beside nucleus
12	Round	14	Round, granular	Lots, clustered around nucleus

**Table 13:** Results taken from Patient #5 (AML) confocal images.

<b>Patient #5: AML Cells</b>				
<b>Image</b>	<b>Cell Morphology</b>	<b>Cell Diameter (µm)</b>	<b>Nuclear Morphology</b>	<b>Mitochondria Morphology</b>
1	Round	10.5	Irregular, lobed, granular	Clustered above/beside nucleus
2	Round	10	Irregular, lobed, granular	Clustered above/beside nucleus
3	Round	10	Irregular, lobed, granular	Clustered beside nucleus
4	Oval	NA	Irregular, lobed, granular	Clustered beside/below nucleus
5	Elongated	NA	Irregular, lobed, granular	Clustered beside nucleus
6	Round	9.5	Irregular, granular	Clustered beside/below nucleus
7	Round	10	Irregular, granular	Clustered above/beside nucleus
8	Oval	NA	Irregular, lobed, granular	Clustered beside nucleus
9	Elongated	NA	Irregular, lobed, granular	Clustered beside nucleus
10	Oval	NA	Irregular, lobed, granular	Clustered beside nucleus
11	Round	10	Irregular, lobed, granular	Clustered beside nucleus
12	Irregular (Oval)	NA	Irregular, granular	Clustered beside/below nucleus
13	Oval	NA	Irregular, lobed, granular	Clustered beside nucleus
14	Round	10	Irregular, granular	Clustered above/beside nucleus
15	Elongated	NA	Irregular, lobed, granular	Clustered beside nucleus
16	Round	10	Irregular, lobed, granular	Clustered above/beside nucleus
17	Irregular (Round)	NA	Irregular, lobed, granular	Clustered around the nucleus
18	Elongated	NA	Irregular, granular	Clustered beside nucleus
19	Round	10.5	Irregular, lobed, granular	Clustered around the nucleus
20	Round	9.5	Irregular, lobed, granular	Clustered beside/below nucleus
21	Elongated	NA	Irregular, granular	Clustered above/beside nucleus
22	Round	9	Irregular, lobed, granular	Clustered beside nucleus
23	Irregular (Round)	NA	Irregular, granular	Clustered beside nucleus
24	Oval	NA	Irregular, lobed, granular	Clustered around the nucleus
25	Round	9.5	Irregular, granular	Clustered beside nucleus
26	Oval	NA	Irregular, lobed, granular	Clustered beside nucleus
27	Oval	NA	Irregular, lobed, granular	Clustered above/beside nucleus

**Table 14:** Results taken from Patient #6 (ALL) confocal images.

<b>Patient #6: ALL Cells</b>				
<b>Image</b>	<b>Cell Morphology</b>	<b>Cell Diameter (µm)</b>	<b>Nuclear Morphology</b>	<b>Mitochondria Morphology</b>
1	Round	8	Irregular, granular	Clustered beside nucleus
2	Round	8.5	Irregular, lobed, granular	Clustered beside nucleus
3	Round	9	Irregular, granular	Clustered beside nucleus
4	Round	8	irregular kidney, granular	Clustered beside nucleus
5	Round	9	Kidney, granular	Clustered beside nucleus
6	Round	9	Irregular, lobed, granular	Clustered beside nucleus
7	Round	8	Irregular, granular	Clustered beside nucleus
8	Round	8.5	Irregular, granular	Clustered beside nucleus
9	Round	7	Irregular, granular	Clustered beside nucleus
10	Round	9	Irregular, granular	Clustered beside nucleus
11	Round	8.5	Oval, granular	Clustered beside nucleus
12	Oval	NA	Kidney, granular	Clustered beside nucleus
13	Round	9	Irregular, lobed, granular	Clustered beside nucleus
14	Round	8	Irregular, lobed, granular	Clustered beside nucleus
15	Round	10	Irregular, lobed, granular	Clustered on 2 sides of nucleus
16	Round	9	Irregular, lobed, granular	Clustered beside nucleus
17	Round	9	Irregular, granular	Clustered beside nucleus
18	Round	8.5	Irregular, lobed, granular	Clustered beside nucleus
19	Round	9	Irregular, granular	Clustered beside nucleus
20	Round	9	Kidney, granular	Clustered beside nucleus

**Table 15:** Summary of results

<b>Cell Line</b>	<b>Cell Morphology</b>	<b>Avg. Cell Diameter (um)</b>	<b>Std. Deviation</b>	<b>Nuclear Morphology</b>	<b>Mitochondrial Distribution</b>	<b>Number of Cells Imaged</b>
Nalm-6	Round	9.73	1.03	Irregular, lobed	Varied	40
Jurkat	Round	9.50	0.91	Round/Ovoid	Clustered in one area beside nucleus	40
HL-60	Round	11.36	0.77	Round	Around nucleus	40
U937	Round	11.79	0.99	Irregular	Varied	40
TPA Stimulated	Round/Ovoid	9.82	0.98	Varied	Clustered in one area beside nucleus	40
PHA Stimulated	Round/Ovoid	10.53	0.95	Irregular	Clustered in one area beside nucleus	20
ALL Patients (2)	Round/Ovoid	8.59	0.59	Irregular	Clustered in one area beside nucleus	41
AML Patients (3)	Round/Ovoid	9.46	1.25	Varied	Varied	61
Undiagnosed Patient	Round/Ovoid	8.19	2.28	Round	Varied	17

When compared with the two ALL cell lines, the mitogen stimulated non-leukemic control cells exhibited a slightly larger size, both between the B- and T-lymphocytes. The overall cell morphology was similar between all of the cell types imaged, with the majority having round to ovoid shaped cells. Nuclear and mitochondrial properties varied among each of the cell types.

Overall cell morphology for the Nalm-6 B-cells and the TPA stimulated B-cells was very similar. Both types were mainly round in shape, with an occasional ovoid shaped cell. The size difference between Nalm-6 and TPA stimulated cells was minor. The average cell diameter for the Nalm-6 cells was  $9.73\mu\text{m}$ , while the average diameter for the TPA cells was  $9.82\mu\text{m}$ , a difference of only  $0.09\mu\text{m}$ . The vast majority of Nalm-6 cells had irregularly shaped granular nuclei, as did a large number (nearly 60%) of the TPA stimulated B-cells. Most of the irregular Nalm-6 nuclei however had lobed protrusions, while only a handful of the TPA cells shared this feature. The mitochondrial distribution between the Nalm-6 and TPA cells was markedly similar as well, with clusters of mitochondria found together located around and beside the nuclei.

While the Jurkat T-cell line and the PHA stimulated T-cells had similar overall cell morphology, both consisting of mostly round cells, there was a significant difference in cell size. The average diameter of a Jurkat cell was  $9.50\mu\text{m}$ ,  $1.03\mu\text{m}$  smaller than the average diameter of  $10.5\mu\text{m}$  for the PHA cells. Nuclei of the Jurkat cell line were mostly granular and round to ovoid in shape, but a few were kidney-shaped. The nuclear morphology of the PHA stimulated cells varied, with cells having round to irregularly shaped nuclei. The mitochondria for both types were typically clustered together in one area of the cell.

## DISCUSSION

Confocal microscopy gives the ability to examine a single cell in three-dimensions by constructing image “slices” of the different layers of a cell. This type of imaging allows users to examine different aspects of cellular morphology, and therefore has extreme potential for biological applications. This study focuses on the application of confocal microscopy to differentiation of leukemic vs. non-leukemic lymphocytes. It was anticipated that with nuclear and mitochondrial staining, morphological differences would be found between different acute lymphoid leukemia (ALL) cell lines, ALL patient blood cells, and non-leukemic donor blood cells.

Many recent studies have focused on using confocal microscopy paired with fluorescent staining to examine the morphological and biochemical features of cancerous cell types. Peters *et al* used confocal imaging to observe the effects of biotinylation of histones in UV exposed Jurkat cells. During the process of apoptosis, clustering of mitochondria, formation of vacuoles, and cell lysis was observed in the Jurkat cells after UV irradiation (Peters 2002). As with in-vitro studies, it has been shown that cellular morphology can also be examined in-vivo with confocal microscopy techniques. It can be used to obtain images of human epithelial tissue in-vivo with micron resolution, providing information about subcellular morphologic and biochemical changes in epithelial cells (Derzek 2000). Other studies show the use of confocal microscopy to follow cell metabolism and other biochemical processes in both cancerous and non-cancerous cells. Using confocal microscopy, the sphingolipid Ceramide-1-P was shown to increase  $Ca^{2+}$  concentration in the Jurkat cell line, with the release of  $Ca^{2+}$  coming from the endoplasmic reticulum (Colina 2005). IgM localization, binding, and transport in chronic lymphoblastic leukemia B-cells was studied with confocal microscopy, which showed that IgM

retention in the endoplasmic reticulum might play a role in defective assembly of the B-cell receptor (Payelle-Brogard 2003).

This study focused solely on the use of confocal microscopy for the differentiation of leukemic cell types based on morphological features. As with other studies, particular parts of the cell were stained with fluorescent dyes so that they would be detected and visible under the microscope. The nuclei and mitochondria of each cell line imaged in this study were stained with Syto-61 and Mitotracker Orange, respectively. Once the images had been taken, the results for each cell line were examined and compared. The images were used to attain general morphological information, such as overall cell morphology, cell diameter, nuclear morphology and mitochondrial distribution. The data suggests that morphological differences between the different types of leukemic cells can be detected using confocal microscopy. For example, the NALM-6 cell line was very distinct from the HL-60 cell line. NALM-6 cells have irregularly shaped nuclei, and mitochondria that cluster in one area, while the HL-60 cells have round nuclei with mitochondria evenly dispersed throughout the cytoplasm, surrounding the nucleus. Differences between the NALM-6 and Jurkat ALL cell lines were also observed. The mitogen stimulated cells closely resembled their respective B- or T-cell line as well, as described above. By creating a database of different types of leukemic cell images, comparison and variability between each type could be detected.

It is evident that there is some variance within the data for each of the different cell types. This could be attributed to several factors, such as the cells being in different stages of the cell cycle. This would cause the cells to have different morphological features, depending on which stage they were in. Synchronization of cell cycle in each cell type could help solve this problem. Another factor could be the angle at which each cell settles on the surface of the slide. Without

being able to build a three-dimensional image from the z-stacks of each individual cell, it can be difficult to picture the overall shape depending on the angle of the cell. For example, a nucleus that appears to be round or spherical in shape could actually be ovoid, if the z-stack slices are perpendicular. The development of software that can build these 3D images from z-stacks, which is in progress, could potentially eliminate this issue, and at the same time be able to attain more valuable data for each cell. Additional potential data includes cell volume, nuclear volume, mitochondrial number, etc.

Another area of improvement could be further identification and separation of the cell types in blood sample cultures. This would not be relevant for the cell lines, but would be for the PHA and TPA stimulated blood culture cells, and the patient blood culture cells. Since blood samples are full of many different types of lymphocytes and other cells, being able to ensure that you are imaging the specific cell you want, a B or T cell for example, would be very beneficial. The use of flow cytometry to identify and separate out the cell type of interest could be employed to address this.

While the dyes used in this study worked well for staining the nuclei and mitochondria, finding a dye that could bind to each structure more specifically would help to produce a cleaner, sharper image, by eliminating any bleeding of the dyes into other areas of the cell. Initial confocal imaging of the Nalm-6 cell line, which was the first cell line to be imaged, with the Syto-61 and Mitotracker-Orange dyes, showed some issues with bleaching of the nuclear dye. Bleaching occurs when a fluorescent dye loses intensity as the confocal lasers scan through the different layers of a specimen. Also, the Mitotracker-Orange mitochondrial dye also infiltrated areas of the cell other than the mitochondria, including the nucleus. This made the confocal images unclear due to the poor separation of the dyes. Another mitochondrial dye, LDS-751,

was tried in place of the Mitotracker-Orange to try and solve this problem. LDS-751 has been shown to bind almost exclusively with mitochondria (Snyder 2001). This dye, however, did not improve the confocal images due to increased graininess in the images, as a result of high gain settings of laser excitation intensity using the imaging control software that were necessary to make the dye visible. Further imaging with the original dyes, Syto-61 and Mitotracker-Orange, with different gain levels and other software settings proved to provide clearer images with more distinct nuclei and mitochondria. Future studies using dyes to stain other parts of the cell, such as the golgi or ER, could help to further differentiate between cell types.

Confocal microscopy is often used in biological applications to study general cellular morphology and processes, such as apoptosis. This is the first study to apply confocal microscopy to differentiation of leukemic cell types. Based on the data from this study, it has been determined that differentiation of some types of cells is possible, based on morphological features. Using confocal microscopy as a tool for differentiation lends itself to several research possibilities for the future. While the major focus of this study was to test the possibility of differentiating between B and T ALL cells, data was collected for a variety of leukemic cell types. Further studies could expand and build upon the results found here, comparing ALL vs. AML, acute vs. chronic leukemia, and so on. The more specific and accurate studies like these can get, the more useful confocal microscopy becomes as a differentiative tool. Ultimately, it could be possible to use this technique to diagnose the type of leukemia a patient has more rapidly than standard procedures.

## CONCLUSIONS

In conclusion, it has been shown in this study that morphological differences between different leukemia cell lines can be detected using confocal microscopy. While recent studies have proven that confocal microscopy is a valuable tool to study different cellular processes, none have specifically focused on using it as a tool for differentiation of cell types. A recent study showed that confocal microscopy is capable of detecting intracellular processes, such as decreased mitochondrial integrity, one of the events occurring during apoptosis (Peters 2002). This study demonstrates that mitochondrial morphology can also be used to help compare between different leukemic cell types. The various types of leukemic cells had different mitochondrial distribution, including the cell lines in which distribution was extremely uniform. Numerous studies have examined the ability of confocal microscopy to be used in-vivo as a diagnostic tool, for cancers such as non-melanoma skin cancer (Rajadhyaksha 2001), gastrointestinal cancer (Inoue 2005), and cervical cancer (Drezek 2000). Typical diagnosis of leukemia is achieved by pathologic examination, cytogenetics, and/or cell counts. Based on the data presented here, differentiating between cell lines is possible using confocal microscopy. While differences between the leukemic cell types examined in this study were observed, differentiating between actual types of leukemia proved to be more difficult, and is not likely possible based solely on the methods used in this study. The data presented here shows the potential of confocal microscopy as a tool for cellular comparison. It also proves that future studies will need to be performed in order to eliminate some of the problems found in this study, and to improve upon the techniques used here. For instance, synchronization of cell cycle would help to eliminate any differences observed within the same cell type due to cells being in different stages. Synchronization would improve the uniformity of the data within the individual

cell type groups, the cell lines, and the leukemic and non-leukemic patient samples. Also, the use of flow cytometry could be applied to ensure the specific cells of interest are isolated from blood samples. Although there was some experimentation with mitochondrial dyes in this study, different dyes could be used to give the cell parts a sharper image. Additional dyes for other cell parts could also be implemented to help comparison. As demonstrated by this study, there is great potential for confocal microscopy for comparison of cells, and with more research, it could be combined with other diagnostic methods to help diagnose types of leukemia.

## REFERENCES:

- Anderson, K., B. Barlogie, C. Bloomfield, R. Dalla-Favera, and W. Wilson. Report of Leukemia, Lymphoma, and Myeloma. 2001. Progress Review Group: National Cancer Institute. Bethesda, MD.
- Arrasmith, C. 2008. "A combined confocal imaging and Raman Spectroscopy microscope for in vivo skin cancer diagnosis." Montana State University. <http://etd.lib.montana.edu/etd/2008/arrasmith/ArrasmithC1208.pdf>
- Bartholdy, B., and P. Matthias. 2004. "Transcriptional control of B cell development and function." *Gene*. Vol 327: 1-23.
- Birnie, G.D. 1988. "The HL60 cell line: a model system for studying human myeloid cell differentiation." *The British Journal of Cancer Supplement*. Vol 9: 41-45.
- Brock, R.S., X.H. Hu, D.A. Weidner, J.R. Mourant, J.Q. Lu. 2006. "Effect of detailed cell structure on light scattering distribution: FDTD study of a B-cell with 3D structure constructed from confocal images." *Journal of Quantitative Spectroscopy & Radiative Transfer*. 102, 25-36.
- Caspers, PJ, GW Lucassen and GJ Puppels. 2003. "Combined In Vivo Confocal Raman Spectroscopy and Confocal Microscopy of Human Skin." *Biophysical Journal*. Vol 85, No 1, 572-580.
- Chirvinsky, DS, DH Lam, XF Zhao, MP Melman and PD Aplan. "Development and characterization of T cell leukemia cell lines established from SCL/LMO1 double transgenic mice." *Leukemia*. Issue 15, 141-147. 2001.
- Clarkson, B., T. Ohkita, K. Ota, and J. Fried. 1967. Studies of Cellular Proliferation in Human Leukemia: I. Estimation of Growth Rates of Leukemic and Normal Hematopoietic Cells in Two Adults with Acute Leukemia Given Single Injections of Tritiated Thymidine. *Journal of Clinical Investigation*. Vol 46 No 4: 506-529.
- Colina, Claudia, Adriana Flores, Cecilia Castillo, Maria del Rosario Garrido, Anita Israel, Reinaldo DiPolo, and Gustavo Benaim. 2005. "Ceramide-1-P induces Ca<sup>2+</sup> mobilization in Jurkat T-cells by elevation of Ins(1,4,5)-P<sub>3</sub> and activation of a store-operated calcium channel." *Biochemical and Biophysical Research Communications*. 336(1): 54-60.
- Dailey, M., G. Marrs, J. Satz, and M. Waite. 1999. Exploring Biological Structure and Function with Confocal Microscopy. *Biological Bulletin*. Vol 197: 115-122.
- Derzek, Rebekah, Tom Collier, Carrie Brookner, Anais Malpica, Ruben Lotan, Rebecca Richards-Kortum, and Michele Follen. 2000. "Laser scanning confocal microscopy of cervical tissue before and after application of acetic acid." *American Journal of Obstetric Gynecology*. Vol 182, Number 5: 1135-1139.

- Drexler, H., H. Quentmeier and R.A.F. MacLeod. 2005. "Cell line models of leukemia." *Drug Discovery Today: Disease Models*. Vol 2, No 1, 51-56.
- Gallagher, R., S. Collins, J. Trujillo, K. McCredie, M. Ahearn, S. Tsai, R. Metzgar, G. Aulakh, R. Ting, F. Ruscetti, R. Gallo. 1979. "Characterization of the continuous, differentiating myeloid cell line (HL-60) from a patient with acute promyelocytic leukemia." *Blood*. Vol 54, Issue 3, 713-733.
- Gao, J., N. Okada, T. Mayumi, and S. Nakagawa. 2008. "Immune Cell Recruitment and Cell-Based System for Cancer Therapy." *Pharmaceutical Research*. Vol. 25, No. 4, April 2008, 752-768.
- Griffiths, Anthony J.F., William M. Gelbart, Jeffery H. Miller, and Richard C. Lweontin. 1999. *Modern Genetic Analysis*. New York: W.H. Freeman and Company. Chapter 15.
- Grimwade, D., H. Walker, F. Oliver, K. Wheatly, C. Harrison, G. Harrison, J. Rees, I. Hann, R. Stevens, A. Burnett, and A. Goldstone. 1998. The Importance of Diagnostic Cytogenetics on Outcome in AML: Analysis of 1,612 Patients Entered Into the MRC AML 10 Trial. *Blood*. Vol 92 No 7: 2322-2333.
- Guilloton, F., A. de Thonel, C. Jean, C. Demur, V. Mansat-De Mas, G. Laurent and A. Quillet-Mary. 2005. "TNF $\alpha$  stimulates NKG2D-mediated lytic activity of acute myeloid leukemic cells." *Leukemia*. 19: 2206-2214.
- Hurwitz, Richard, John Hozier, Tucker LeBien, Jun Minowada, Kazimiera Gajl-Peczalska, Ichiro Kubonishi, and John Kersey. 1979. "Characterization of a leukemic cell line of the pre-B phenotype." *International Journal of Cancer*. Vol 23, Issue 2, 174-180.
- Inoue, H., S. Kudo and A. Shiokawa. 2004. "Novel Endoscopic Imaging Techniques toward in vivo Observation of Living Cancer Cells in the Gastrointestinal Tract." *Digestive Diseases*. Vol 22, No 4, 334-337.
- Kim, Peter, Peter Lee, and Doron Levy. 2008. "Dynamics and Potential Impact of the Immune Response to Chronic Myelogenous Leukemia." *PLoS Computational Biology*. Vol. 4 Issue 6, 1-17.
- LeBien, T., J. Kersey, S. Nakazawa, K. Minato, and J. Minowada. 1982. Analysis of human leukemia/lymphoma cell lines with monoclonal antibodies BA-1, BA-2 and BA-3. *Leukemia Research*. Vol 6 No 3: 299-305.

- Lee, S., M. Kukreja, T. Wang, S. Giralt, J. Szer, M. Arora, A. Woolfrey, F. Cervantes, R. Champlin, R. Gale, J. Halter, A. Keating, D. Marks, P. McCarthy, E. Olavarria, E. Stadtmauer, M. Abecasis, V. Gupta, H. Khoury, B. George, G. Hale, J. Liesveld, D. Rizzieri, J. Antin, B. Bolwell, M. Carabasi, E. Copelan, O. Ilhan, M. Litzow, H. Schouten, A. Zander, M. Horowitz, and R. Maziarz. 2008. "Impact of prior imatinib mesylate on the outcome of hematopoietic cell transplantation for chronic myeloid leukemia." *Blood*. 15 October 2008, Vol. 112, No. 8, pp. 3500-3507.
- Lilleyman, JS, IM Hann, RF Stevens, OB Eden and SM Richards. 1986. "French American British (FAB) morphological classification of childhood lymphoblastic leukaemia and its clinical importance." *Journal of Clinical Pathology*. 1986;39:998-1002.
- Minowada, J., M. Oshimura, S. Abe, M. Greaves, G. Janossy and A. Sandberg. 1978. "Human leukemia cell lines: Evidence for differentiation toward T- and B-cell axis within a leukemia." *Proceedings of the American Association for Cancer Research*. 19, 109.
- Payelle-Brogard, B., C. Magnac, P. Opezzo, G. Dumas, G. Dighiero and F. Vuillier. 2003. "Retention and defective assembly of the B-cell receptor in the endoplasmic reticulum of chronic lymphocytic leukaemia B cells cannot be reverted upon CD40 ligand stimulation." *Leukemia*. 17,1196-1198.
- Peters, Dorothea, Jacob Griffin, J Steven Stanley, Mary Beck, and Janos Zempleni. 2002 "Exposure to UV light causes increased biotinylation of histiones in Jurkat cells." *American Journal of Physiology-Cell Physiology*. Vol. 283, Issue 3: 878- 884.
- Prasad, V., D. Semwogerere, and ER Weeks. 2007. Confocal microscopy of colloids. *Journal of Physics: Condensed Matter*. Vol 19: 1-25.
- Rajadhyaksha, M., G. Menaker, T. Flotte, PJ Dwyer, S. Gonzalez. 2001. "Confocal examination of nonmelanoma cancers in thick skin excisions to potentially guide mohs micrographic surgery without frozen histopathology." *The Journal of Investigative Dermatology*. Vol 117, No 5, 1137-1143.
- Schneider, Ulrich, Hans-Ulrich Schwenk, and Georg Bornkamm. 1977. "Characterization of EBV-genome negative "null" and "T" cell lines derived from children with acute lymphoblastic leukemia and leukemic transformed non-Hodgkin lymphoma." *International Journal of Cancer*. 19: 621-626.
- Schumacher, HR, IE Szekely, and DR Fisher. 1975. Leuchemic Mitochondria III: Acute Lymphoblastic Leukemia. *American Journal of Pathology*. Vol 78 No 1: 49-56.
- Semwogerere, Denis, and Eric R. Weeks. 2005. Confocal microscopy. *Encyclopedia of Biomaterials and Biomedical Engineering*. Taylor and Francis. Pgs 1-10.
- Singh, A., K.P. Gopinathan. 1998. "Confocal microscopy: A powerful technique for biological research." *Current Science*. Vol 74, No 10, 841-851.

- Smits, E., Z. Berneman, V. Van Tendeloo. 2009. "Immunotherapy of Acute Myeloid Leukemia: Current Approaches." *The Oncologist*. Vol. 14, No. 3, 240-252, March 2009.
- Snyder, D.S., P.L. Small. 2001. "Staining of cellular mitochondria with LDS-751." *Journal of Immunological Methods*. Vol 257, Issue 1-2, 35-40.
- Sundstrom, C., K. Nilsson. 1976. "Establishment and characterization of a human histiocytic lymphoma cell line (U-937)." *International Journal of Cancer*. Vol 17, Issue 5, 565-577.
- Wadleigh, Martha, Daniel DeAngelo, James Griffin and Richard Stone. 2005. "After chronic myelogenous leukemia: tyrosine kinase inhibitors in other hematologic malignancies." *Blood*. Vol. 105, Number 1: 22-30.
- Zhang, Chunyang, Yanping Li, Hui Ma, Suwen Li, Shaobai Xue, and Dieyan Chen. 2001. "Simultaneous multi-parameter observation of Harringtonine-treating HL-60 cells with both two-photon and confocal laser scanning microscopy." *Science in China*. Vol 44, No 4: 383-391.

**APPENDIX A: MINIMUM ESSENTIAL MEDIA**

Minimum Essential Media (MEM) Recipe: (For use with Nalm-6 cells)

175 mL Minimal Essential Media

20 mL Fetal Bovine Serum

2 mL Penicillin/Streptomycin

2 mL L-Glutamine

**APPENDIX B: RPMI MEDIUM**

Roswell Park Memorial Institute (RPMI) Media Recipe: (For use with HL-60 and U937 cells)

500 mL RPMI + GlutaMax-1

5 mL Sodium Pyruvate

5 mL 1 molar HEPES pH 7.5

50 mL Fetal Bovine Serum

**APPENDIX C: REPRESENTATIVE IMAGES COLLECTED OF EACH CELL TYPE**

**NALM-6 Cell Line – Cell #13**

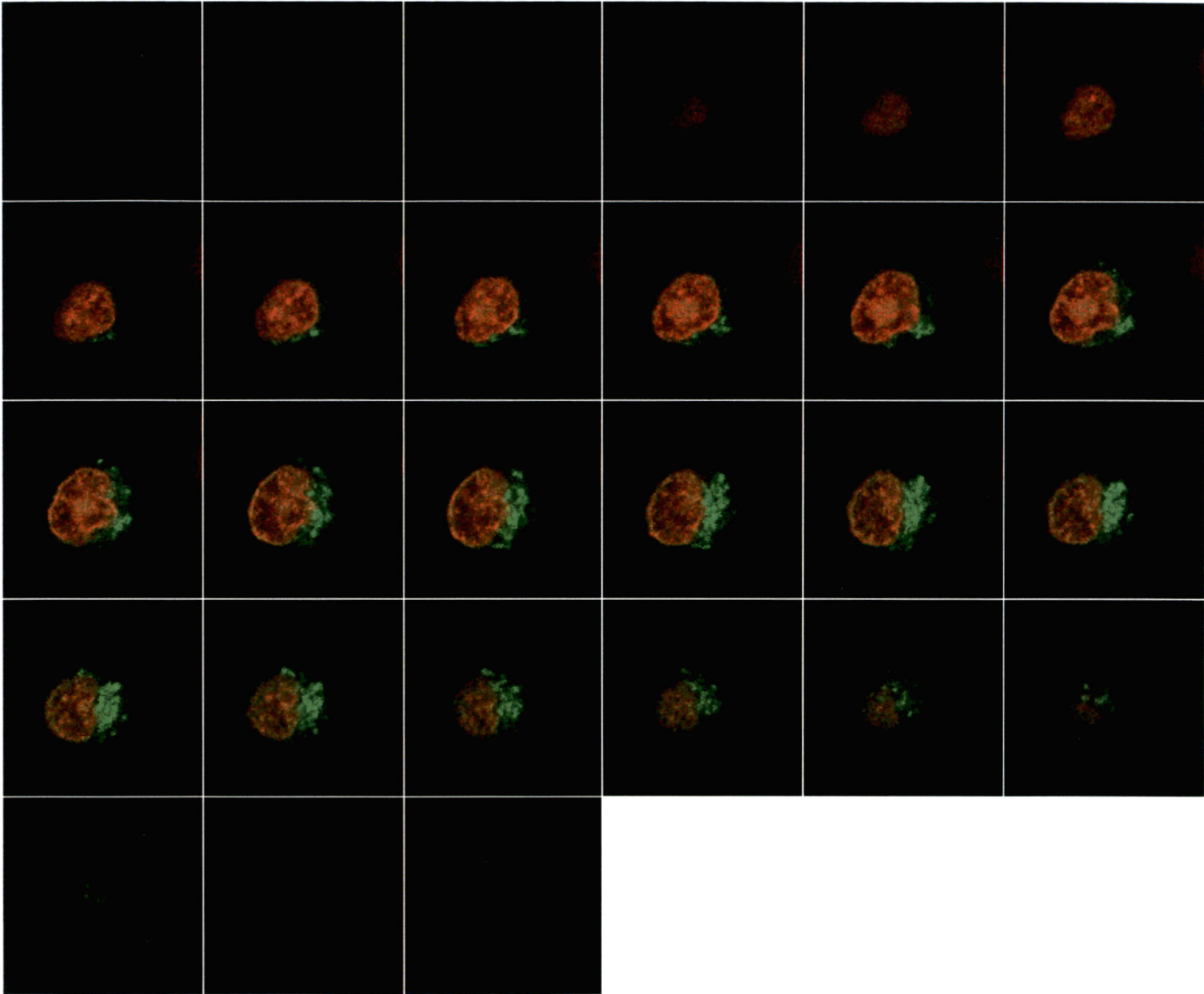


Image #	Date Taken	Saved As	Cell Morphology	Cell Diameter (um)	Nuclear Morphology	Mitochondria Morphology
13	7/23/2008	NALM-6 #9	Round	11.5	Irregular, lobed, granular	Clustered beside and below nucleus

## NALM-6 Cell Line – Cell #13

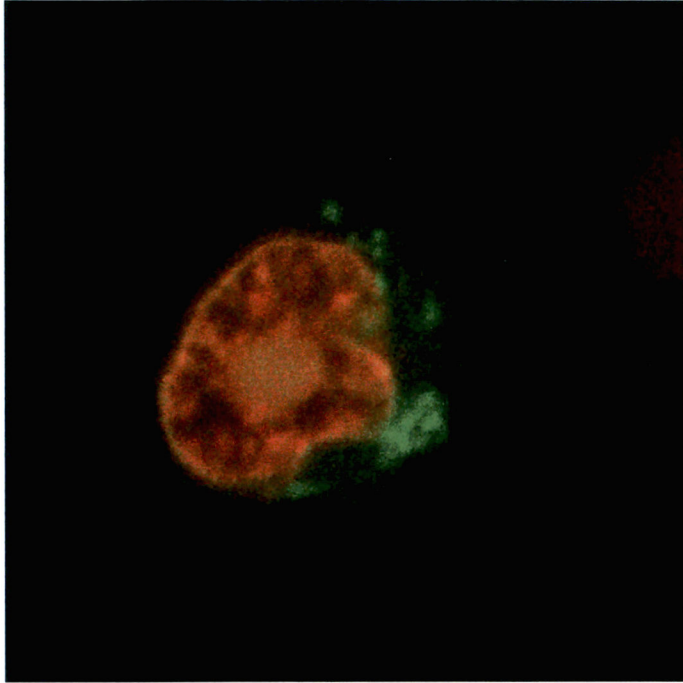


Image #	Cell Line	Slice #	Date Taken
13	NALM-6	12	7/23/08

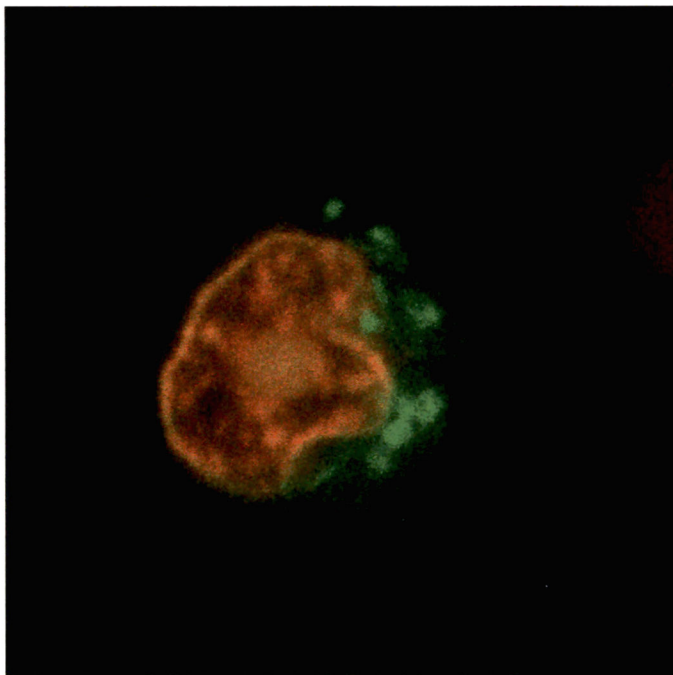


Image #	Cell Line	Slice #	Date Taken
13	NALM-6	13	7/23/08

## NALM-6 Cell Line – Cell #34

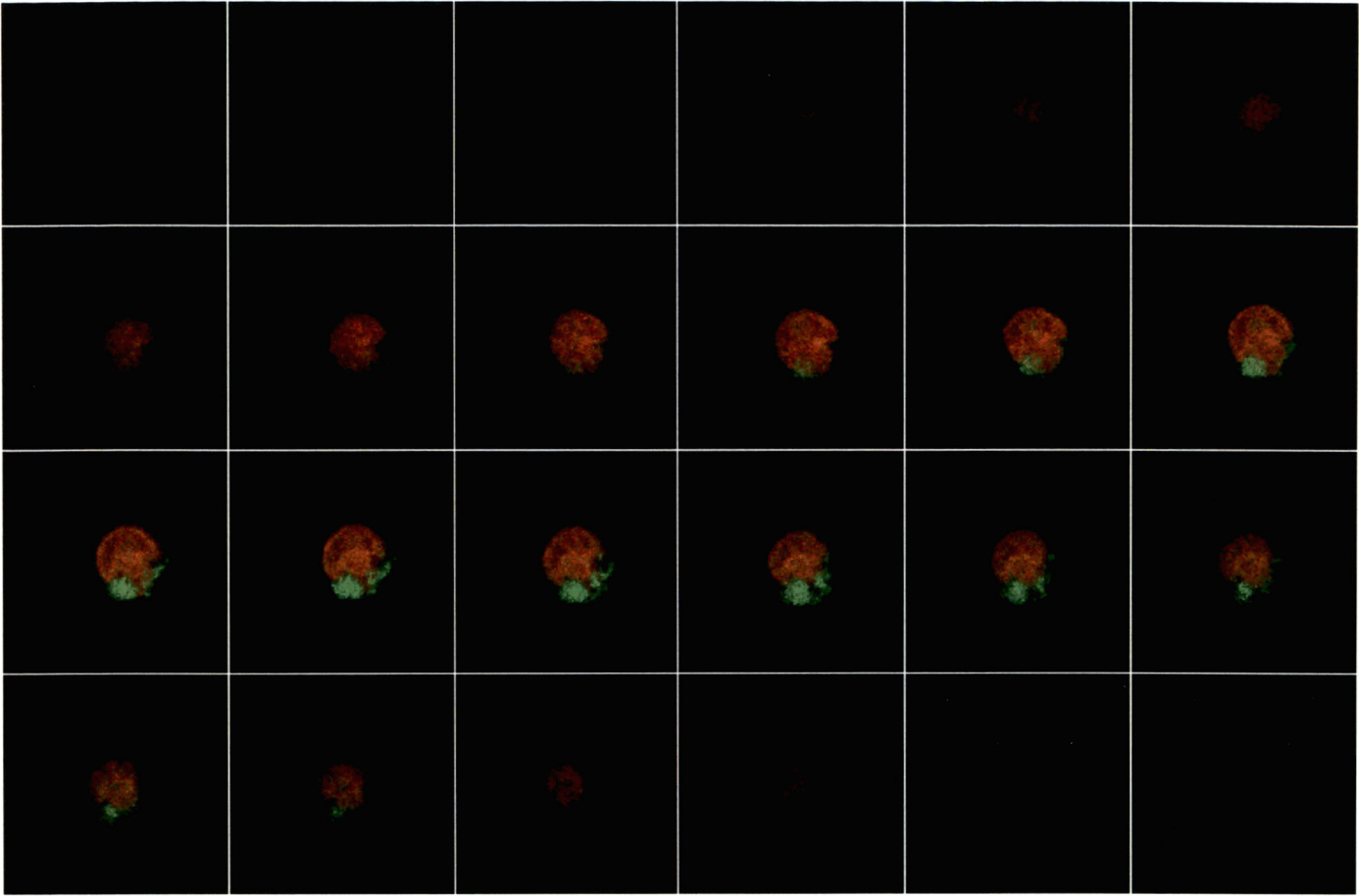
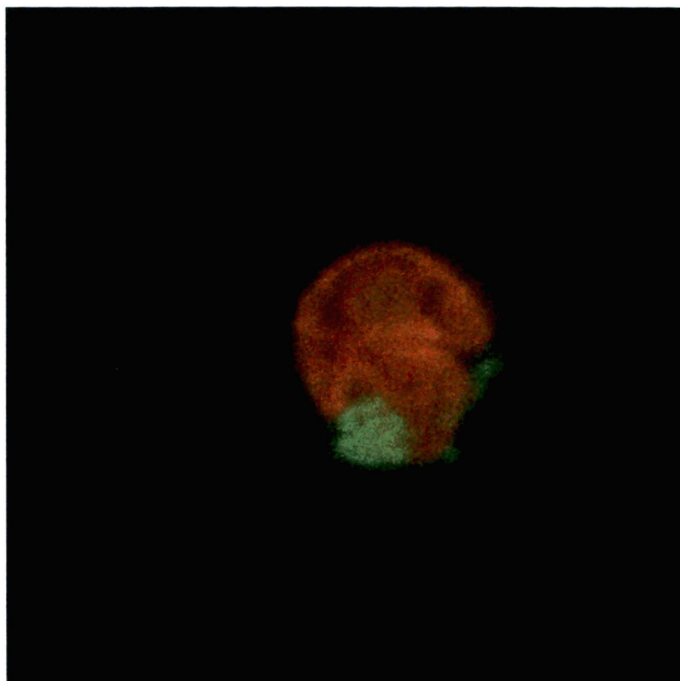
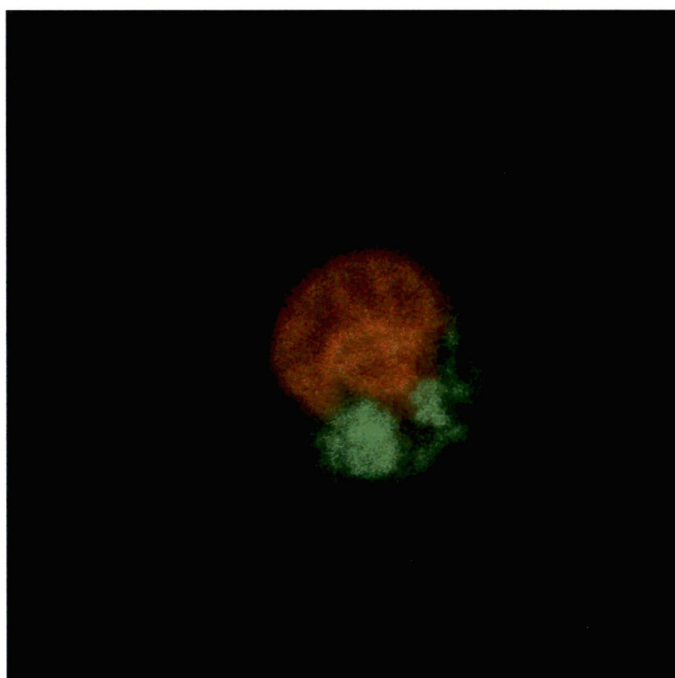


Image #	Date Taken	Saved As	Cell Morphology	Cell Diameter (um)	Nuclear Morphology	Mitochondria Morphology
34	8/22/2008	NALM-6 #4	Round	8.5	Irregular, lobed, granular	Clustered beside nucleus

**NALM-6 Cell Line – Cell #34**

<b>Image #</b>	<b>Cell Line</b>	<b>Slice #</b>	<b>Date Taken</b>
34	NALM-6	12	8/22/08



<b>Image #</b>	<b>Cell Line</b>	<b>Slice #</b>	<b>Date Taken</b>
34	NALM-6	16	8/22/08

PHA Stimulated T-Cells – Cell #5

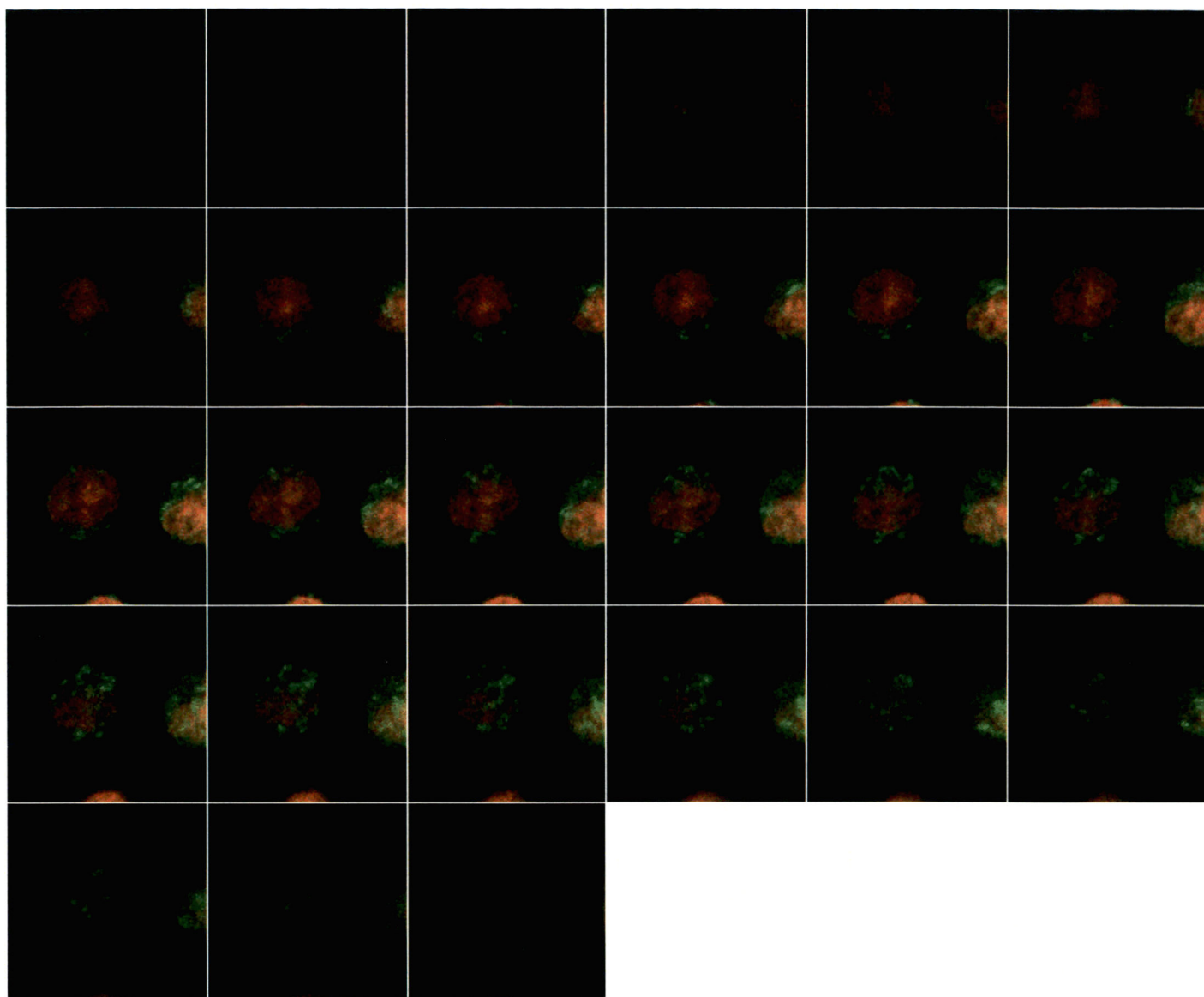
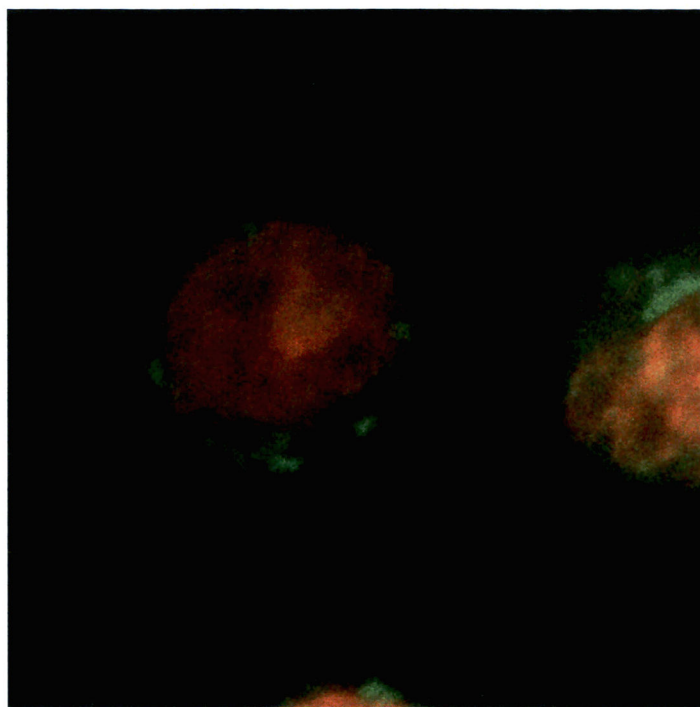
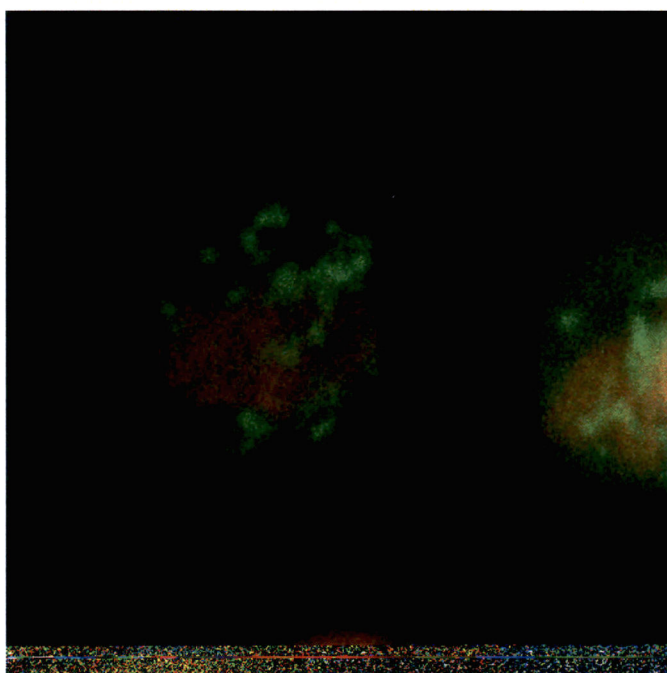


Image #	Date Taken	Saved As	Cell Morphology	Cell Diameter (um)	Nuclear Morphology	Mitochondria Morphology
5	10/16/2008	PHA Cell #4	Round	11.0	Round, granular	Clustered below nucleus

**PHA Stimulated T-Cells – Cell #5**

<b>Image #</b>	<b>Cell Line</b>	<b>Slice #</b>	<b>Date Taken</b>
5	PHA Stimulated Cells	11	10/16/08



<b>Image #</b>	<b>Cell Line</b>	<b>Slice #</b>	<b>Date Taken</b>
5	PHA Stimulated Cells	20	10/16/08

PHA Stimulated T-Cells – Cell #14

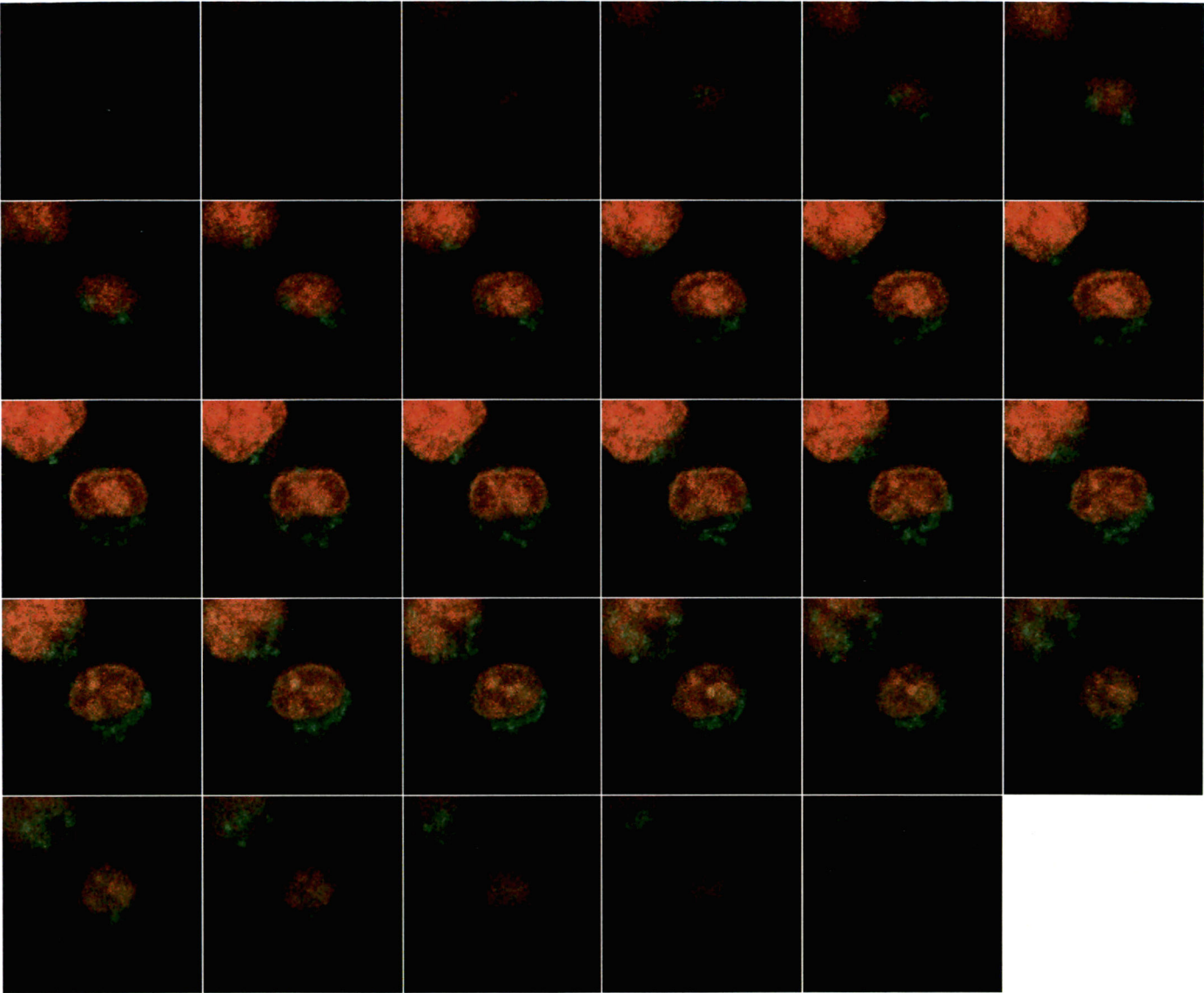
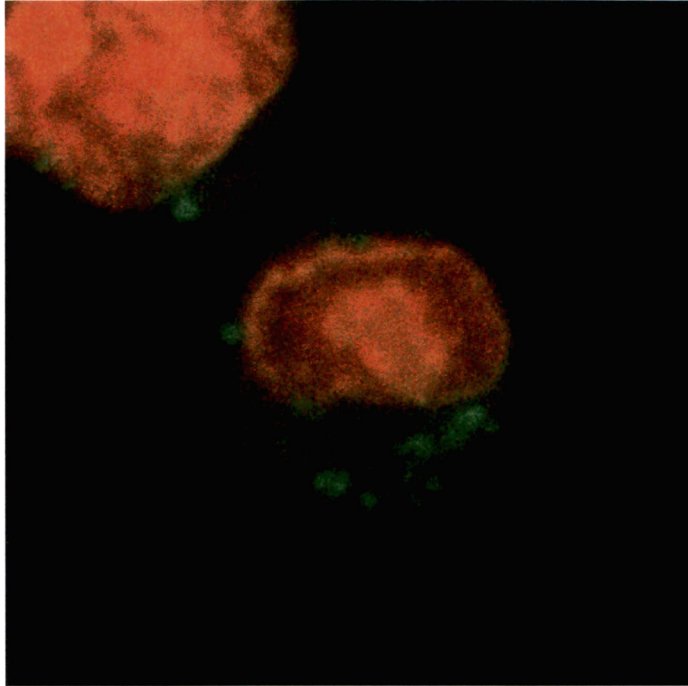
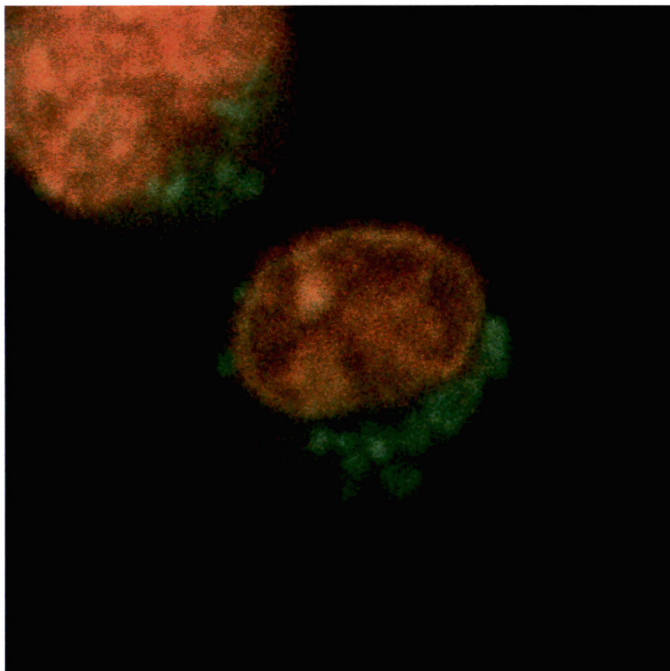


Image #	Date Taken	Saved As	Cell Morphology	Cell Diameter (um)	Nuclear Morphology	Mitochondria Morphology
14	10/16/2008	PHA Cell #14	Round	11.0	Oval, granular	Clustered beside nucleus

**PHA Stimulated T-Cells – Cell #14**

<b>Image #</b>	<b>Cell Line</b>	<b>Slice #</b>	<b>Date Taken</b>
14	PHA Stimulated Cells	12	10/16/08



<b>Image #</b>	<b>Cell Line</b>	<b>Slice #</b>	<b>Date Taken</b>
14	PHA Stimulated Cells	19	10/16/08

## TPA Stimulated B-Cells – Cell #11

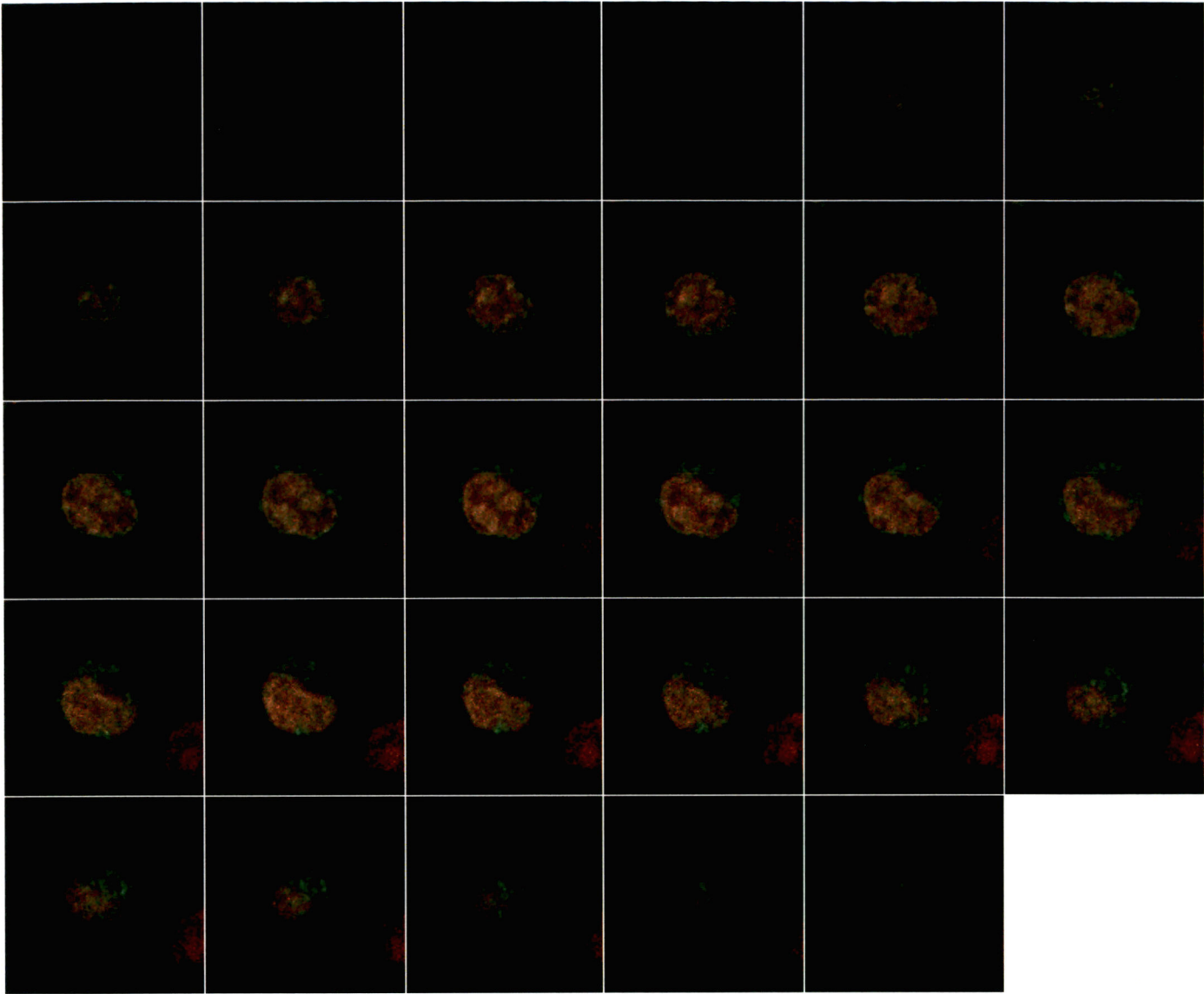
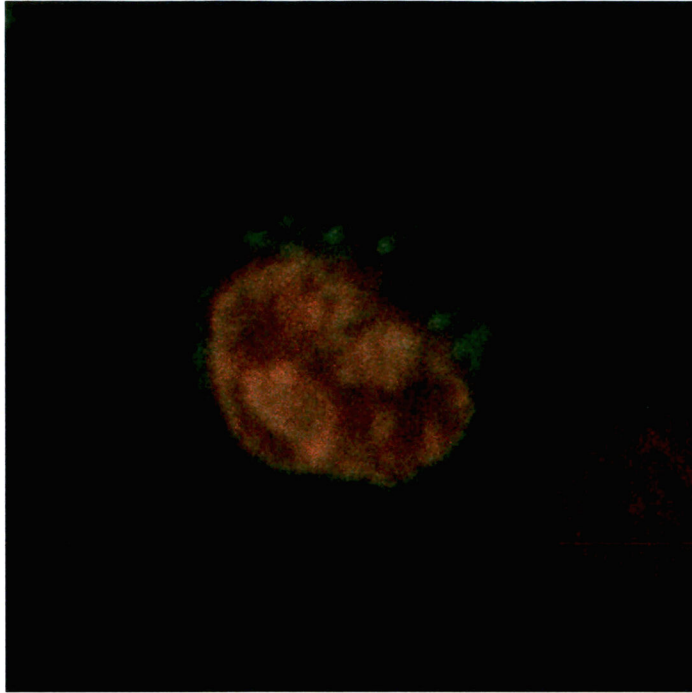
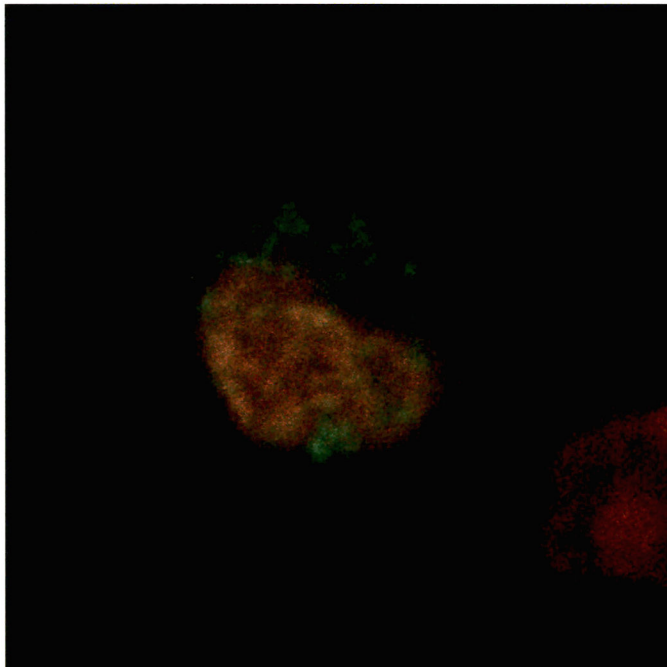


Image #	Date Taken	Saved As	Cell Morphology	Cell Diameter (um)	Nuclear Morphology	Mitochondria Morphology
11	10/16/2008	TPA Cell #14	Round	11.0	Irregular, lobed, granular	Clustered beside/below nucleus

**TPA Stimulated B-Cells – Cell #11**



<b>Image #</b>	<b>Cell Line</b>	<b>Slice #</b>	<b>Date Taken</b>
11	TPA Stimulated Cells	15	10/16/08



<b>Image #</b>	<b>Cell Line</b>	<b>Slice #</b>	<b>Date Taken</b>
11	TPA Stimulated Cells	21	10/16/08

## TPA Stimulated B-Cells – Cell #31

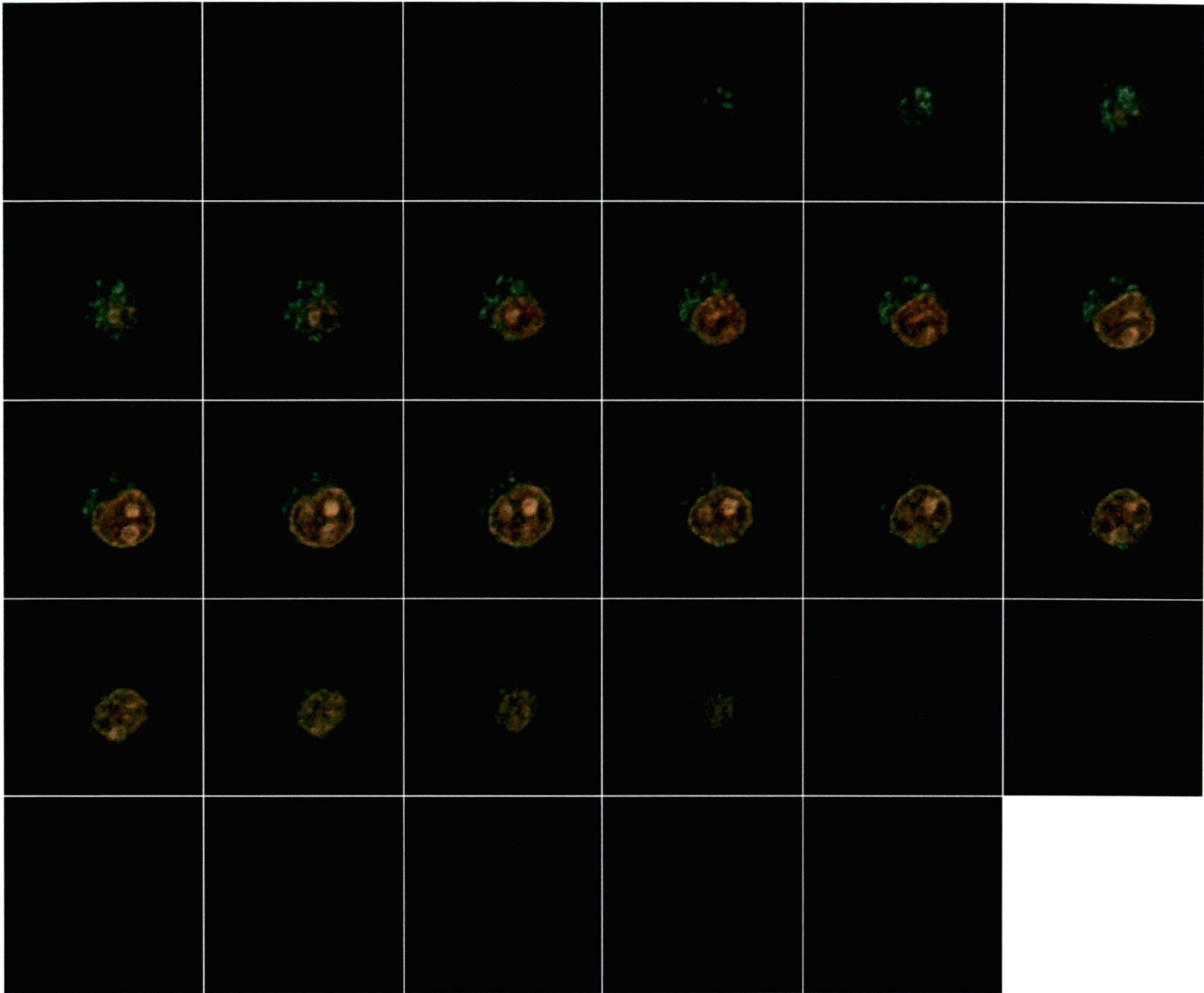
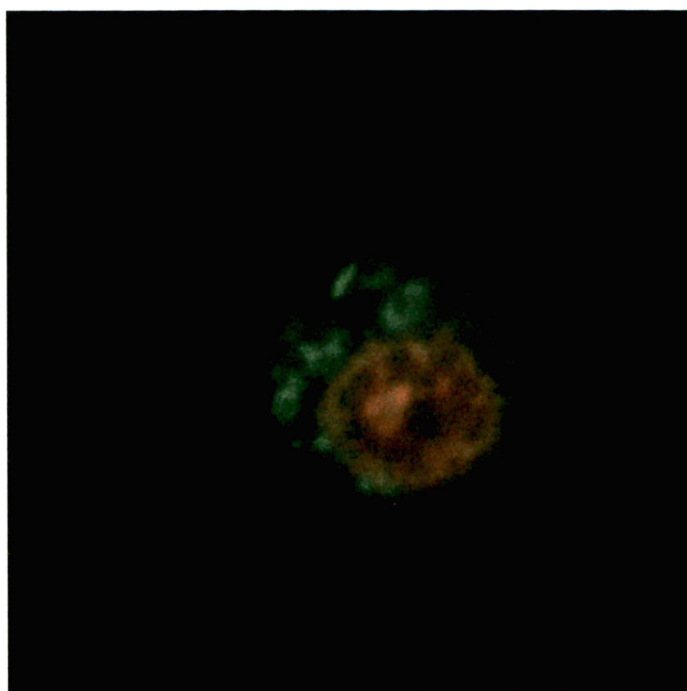
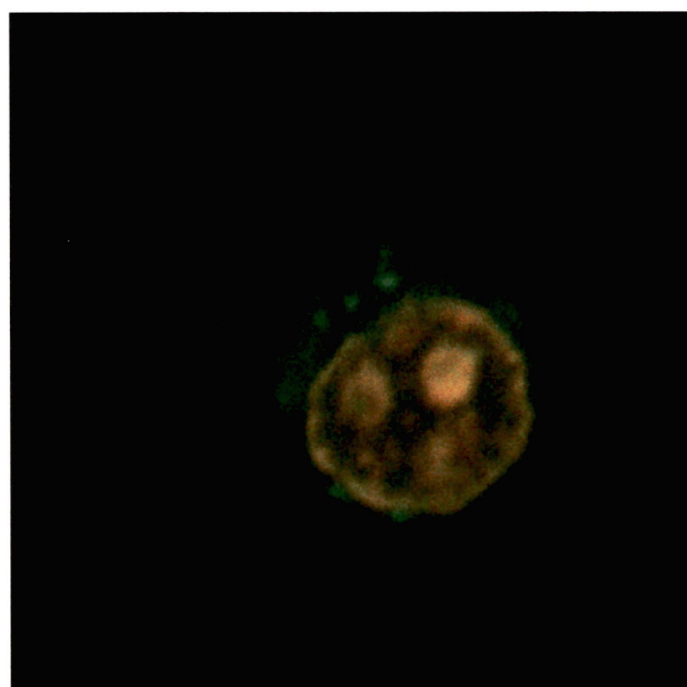


Image #	Date Taken	Saved As	Cell Morphology	Cell Diameter (um)	Nuclear Morphology	Mitochondria Morphology
31	11/21/2008	TPA #15	Round	10.0	Round, granular	Clustered above/beside nucleus

**TPA Stimulated B-Cells – Cell #31**

<b>Image #</b>	<b>Cell Line</b>	<b>Slice #</b>	<b>Date Taken</b>
31	TPA Stimulated Cells	9	11/21/08



<b>Image #</b>	<b>Cell Line</b>	<b>Slice #</b>	<b>Date Taken</b>
31	TPA Stimulated Cells	15	11/21/08

## Jurkat Cell Line – Cell #14

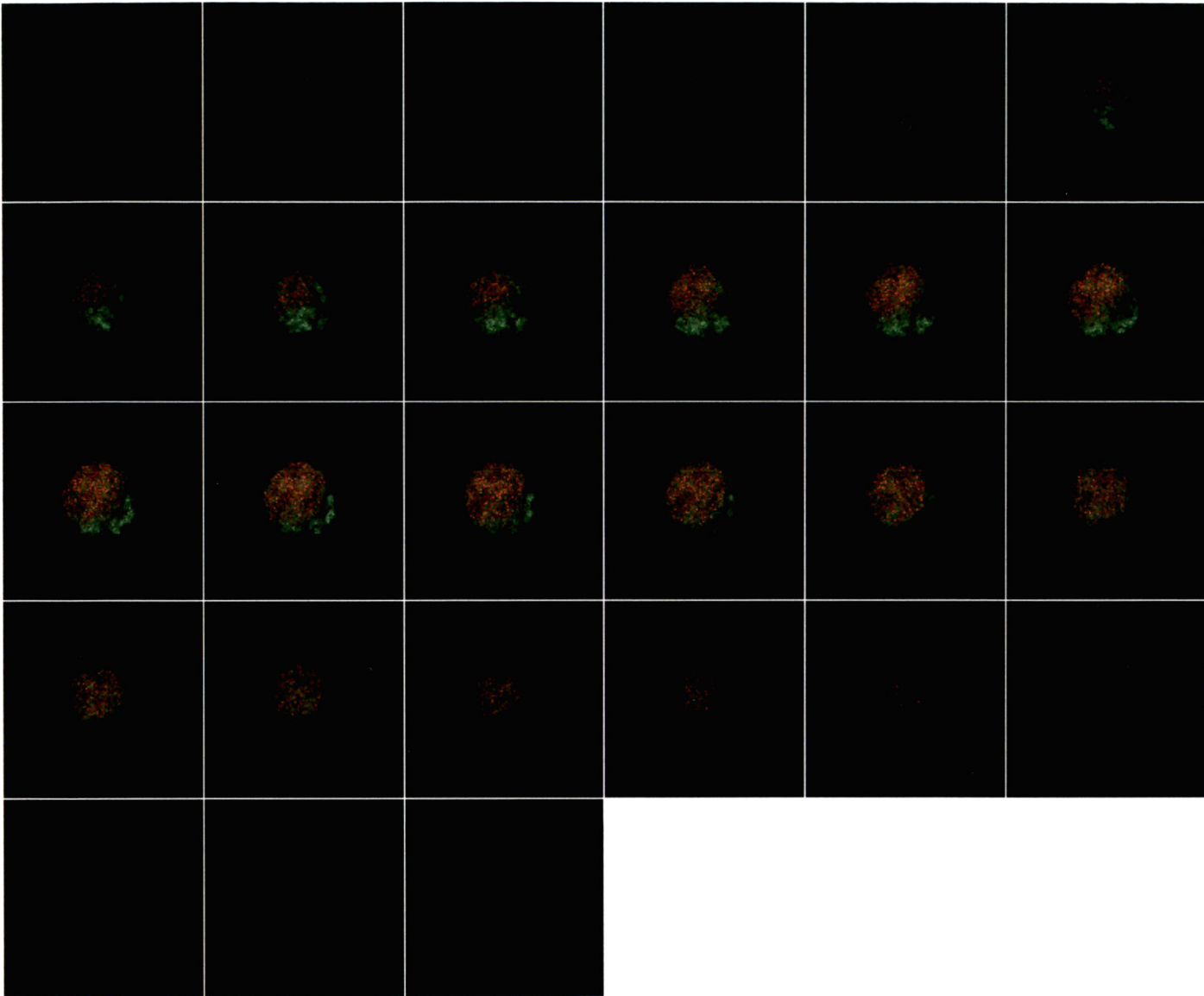
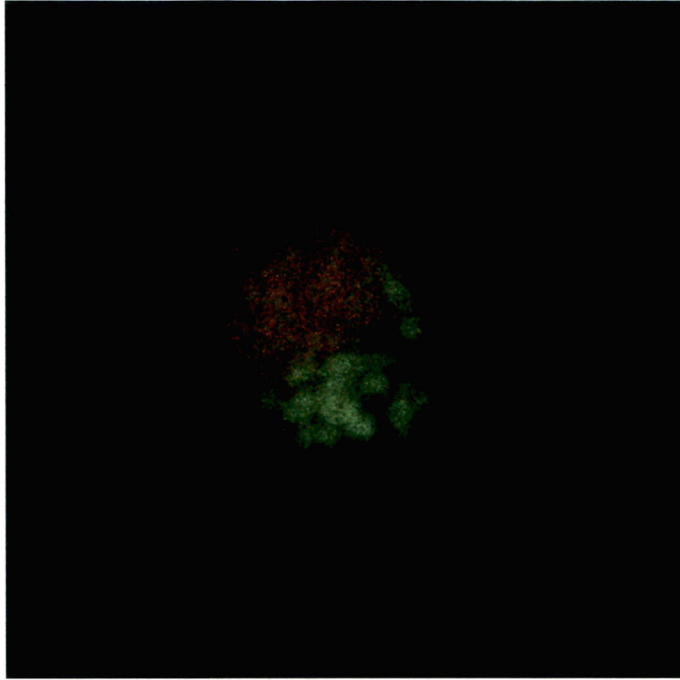
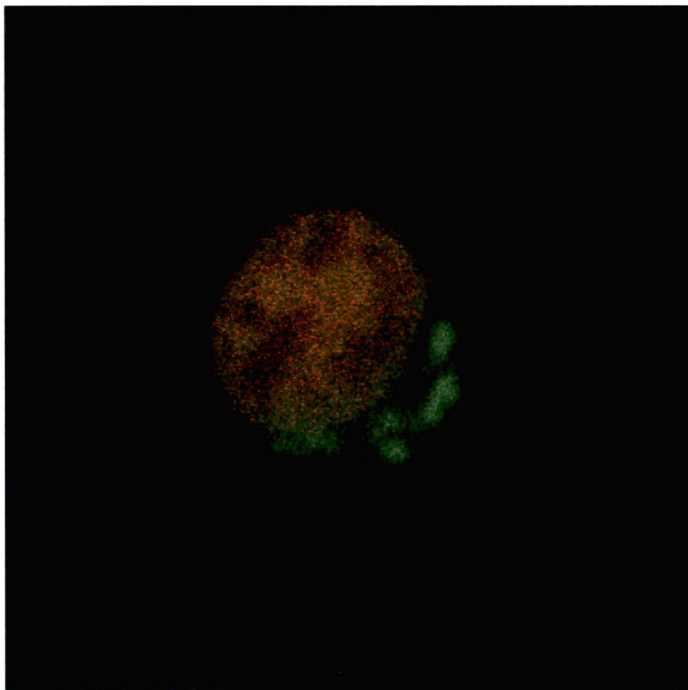


Image #	Date Taken	Saved As	Cell Morphology	Cell Diameter (um)	Nuclear Morphology	Mitochondria Morphology
14	8/19/2008	Jurkat #6	Round	9.0	Round, granular	Clustered beside nucleus

**Jurkat Cell Line – Cell #14**

<b>Image #</b>	<b>Cell Line</b>	<b>Slice #</b>	<b>Date Taken</b>
14	Jurkat	8	8/19/08



<b>Image #</b>	<b>Cell Line</b>	<b>Slice #</b>	<b>Date Taken</b>
14	Jurkat	14	8/19/08

## Jurkat Cell Line – Cell #24

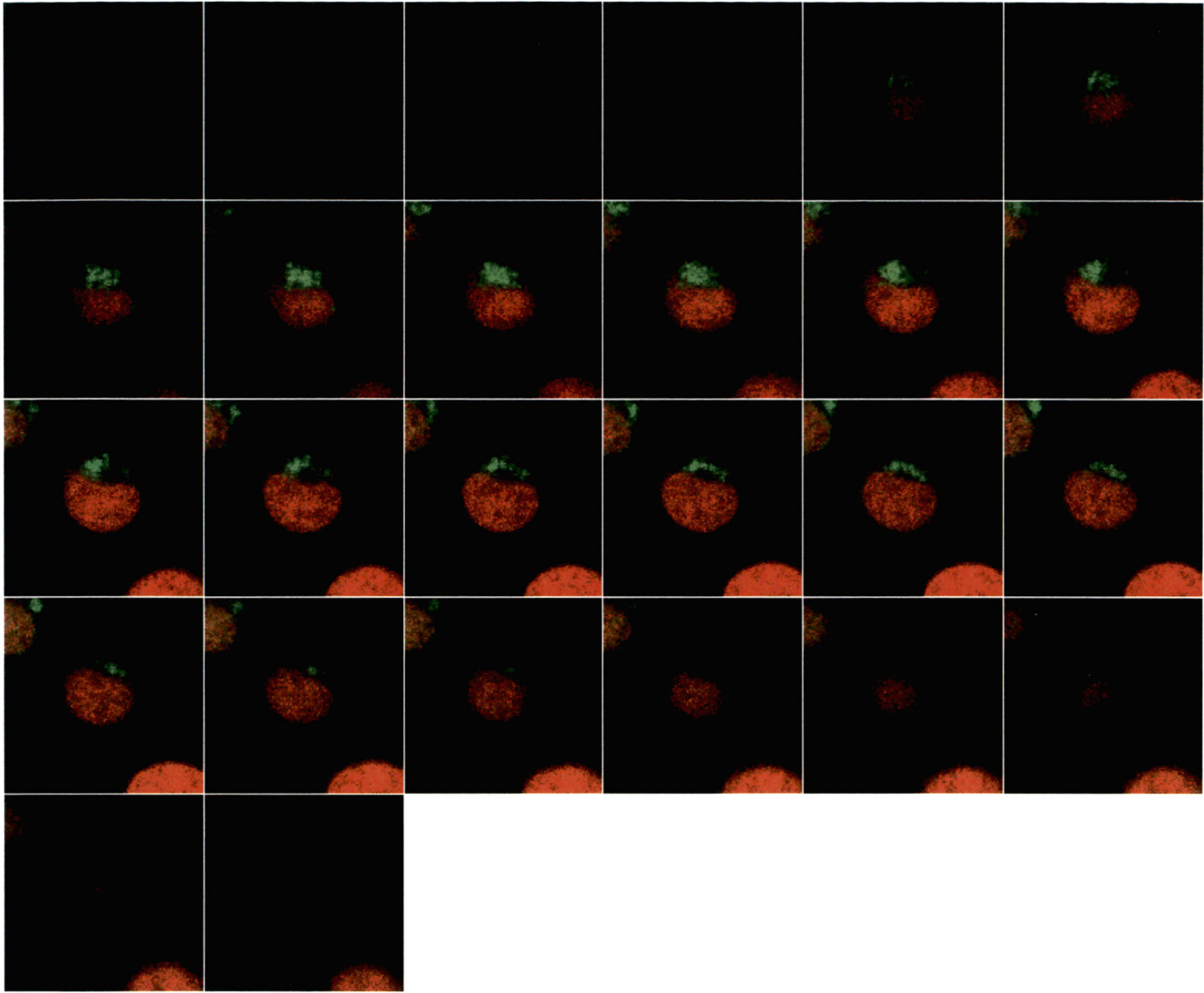
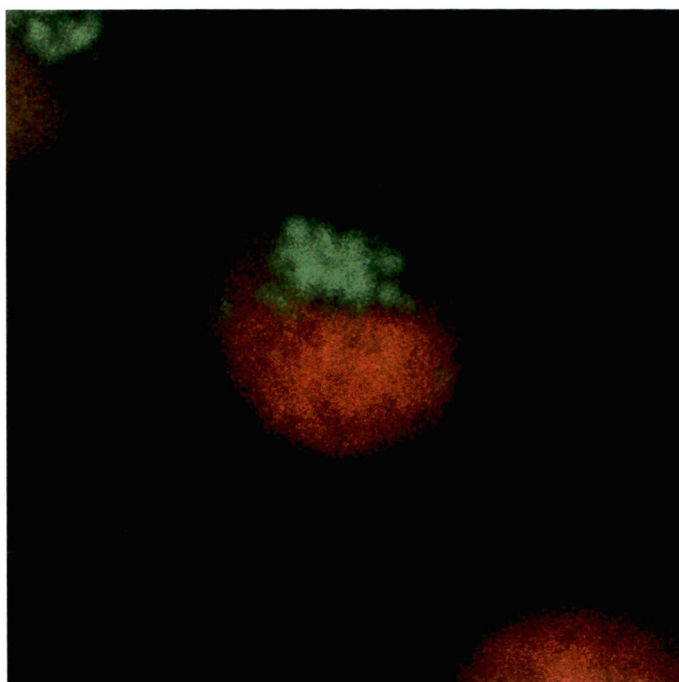
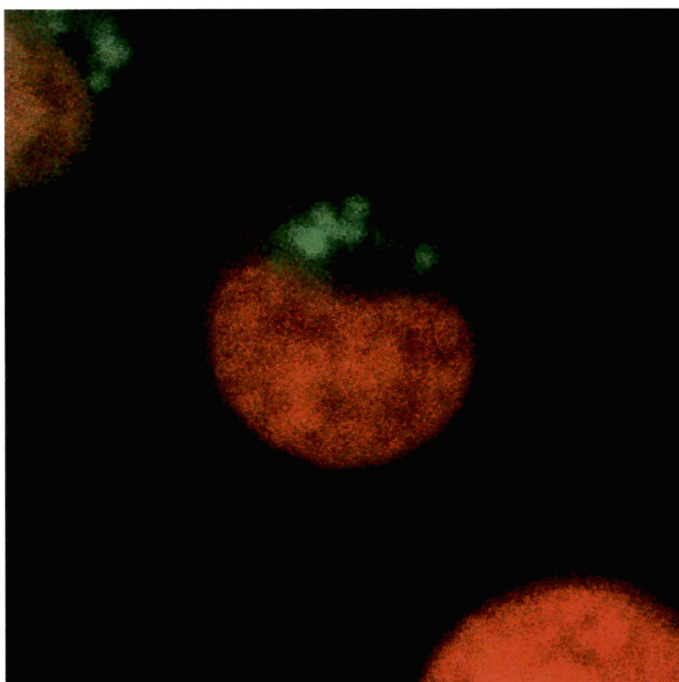


Image #	Date Taken	Saved As	Cell Morphology	Cell Diameter (um)	Nuclear Morphology	Mitochondria Morphology
24	8/22/2008	Jurkat #6	Round	10.0	Kidney, granular	Clustered beside nucleus

**Jurkat Cell Line – Cell #24**

<b>Image #</b>	<b>Cell Line</b>	<b>Slice #</b>	<b>Date Taken</b>
24	Jurkat	9	8/22/08



<b>Image #</b>	<b>Cell Line</b>	<b>Slice #</b>	<b>Date Taken</b>
24	Jurkat	14	8/22/08

## HL60 Cell Line – Cell #26

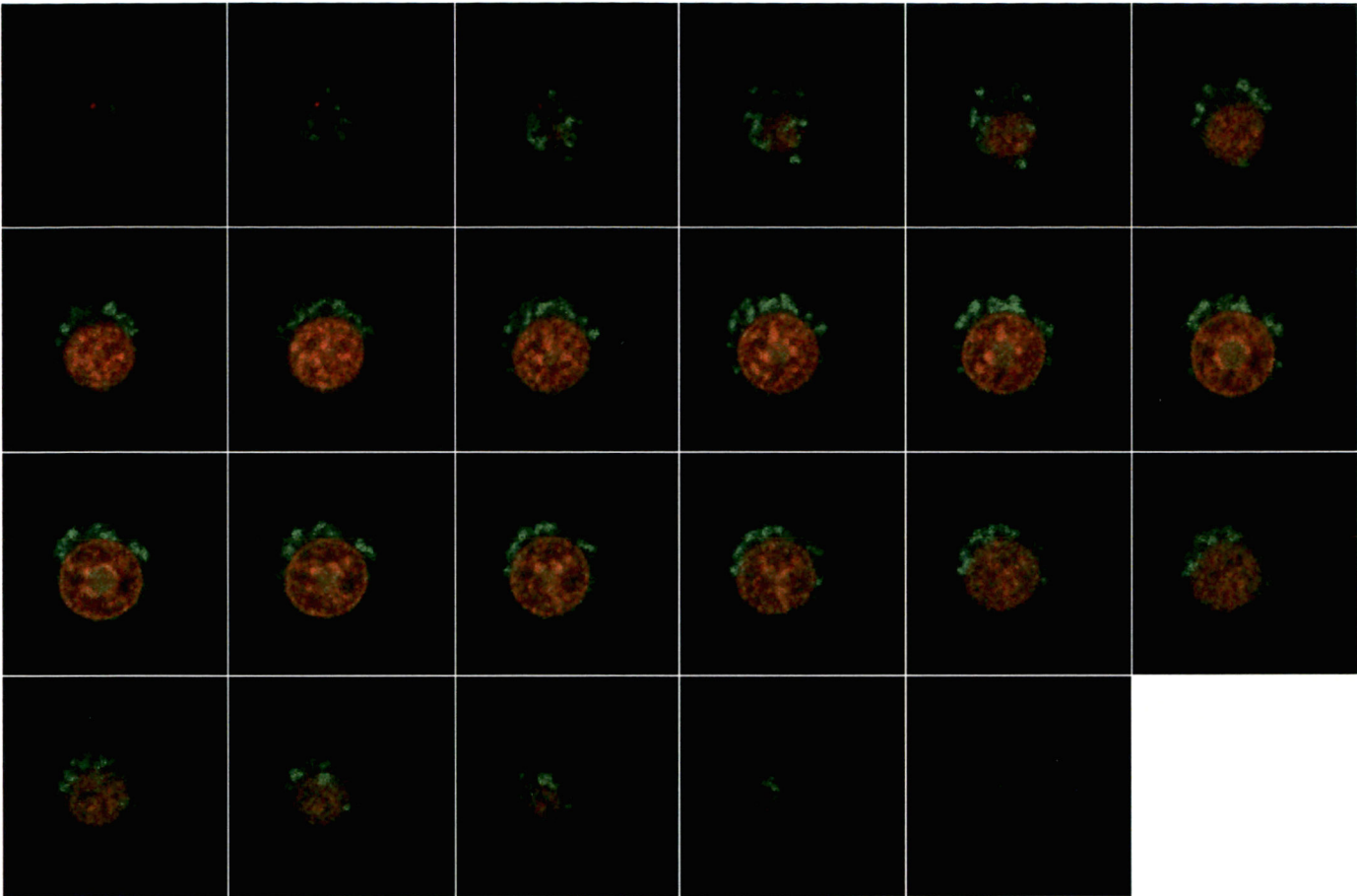
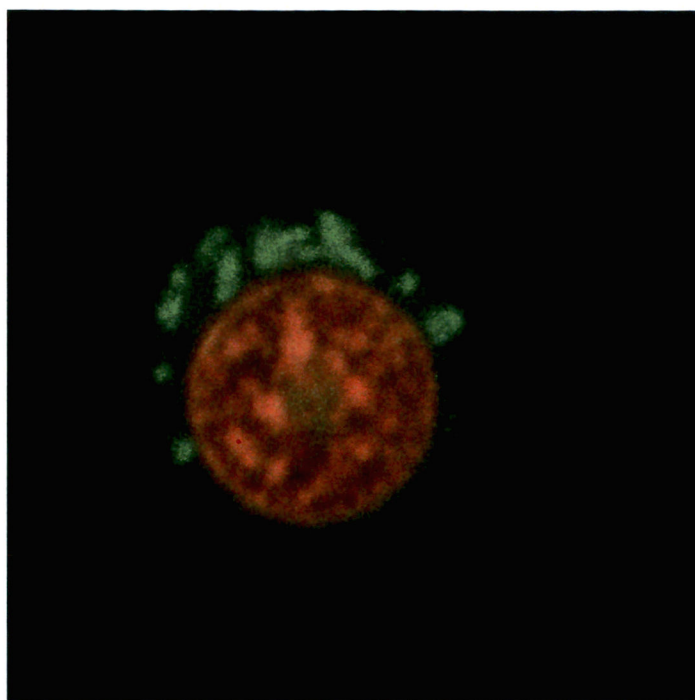
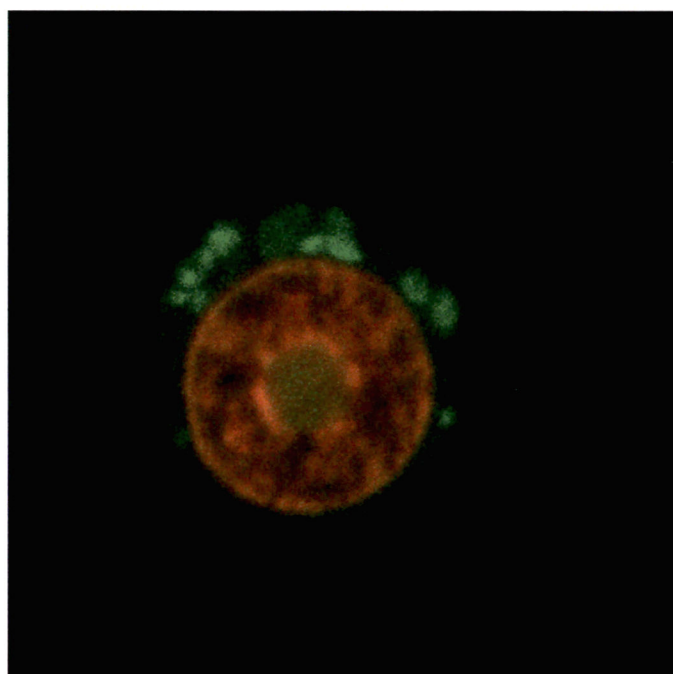


Image #	Date Taken	Saved As	Cell Morphology	Cell Diameter (um)	Nuclear Morphology	Mitochondria Morphology
26	7/16/2008	HL60 #6	Round	11	Round granular	Clustered around nucleus

**HL60 Cell Line – Cell #26**

<b>Image #</b>	<b>Cell Line</b>	<b>Slice #</b>	<b>Date Taken</b>
26	HL60	10	7/16/08



<b>Image #</b>	<b>Cell Line</b>	<b>Slice #</b>	<b>Date Taken</b>
26	HL60	12	7/16/08

## HL60 Cell Line – Cell #29

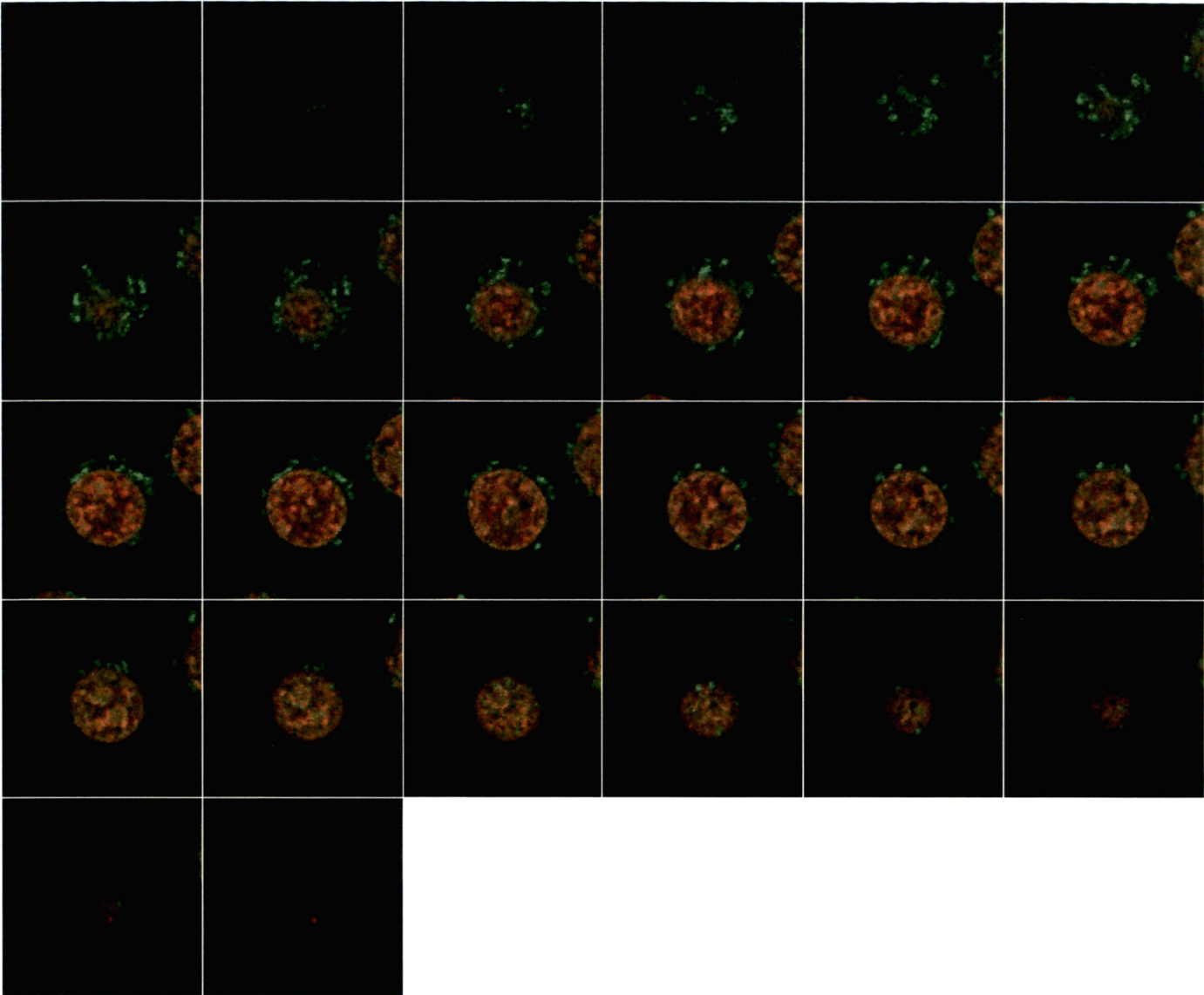
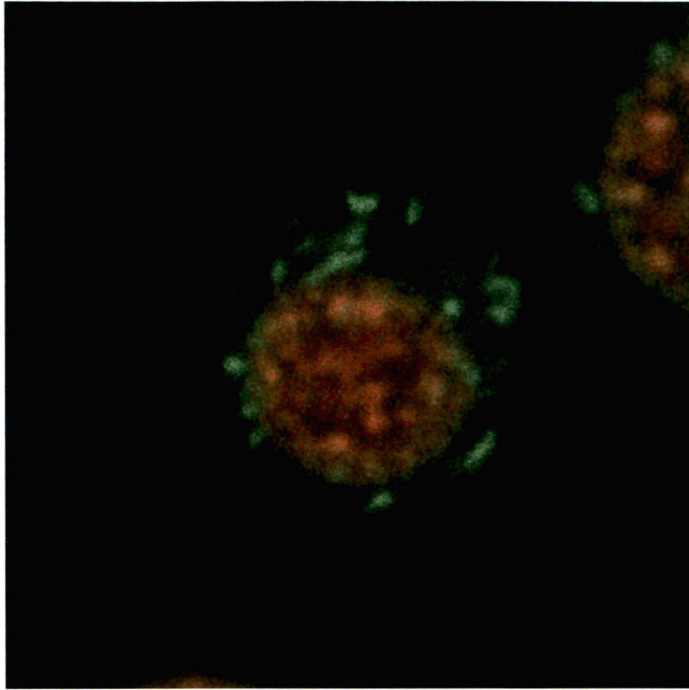
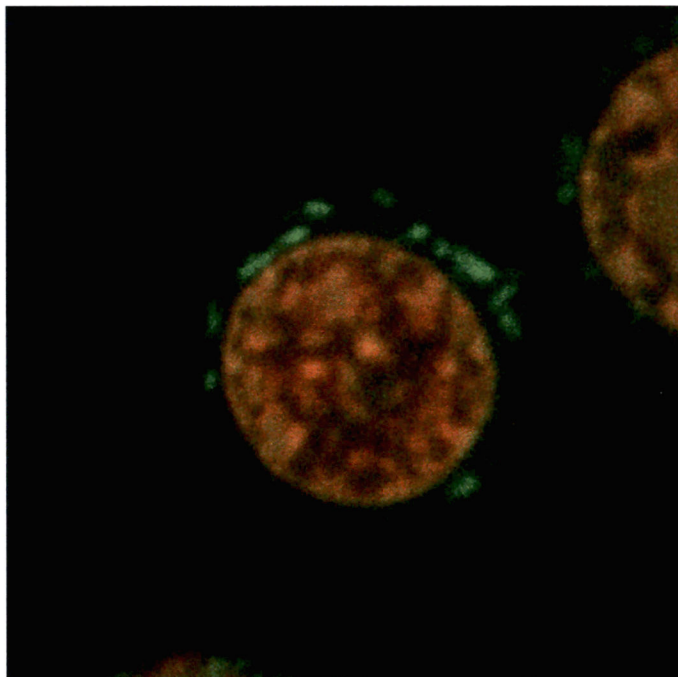


Image #	Date Taken	Saved As	Cell Morphology	Cell Diameter (um)	Nuclear Morphology	Mitochondria Morphology
29	7/16/2008	HL60 #9	Round	11.5	Round granular	Clustered above/beside nucleus

**HL60 Cell Line – Cell #29**

<b>Image #</b>	<b>Cell Line</b>	<b>Slice #</b>	<b>Date Taken</b>
29	HL60	9	7/16/08



<b>Image #</b>	<b>Cell Line</b>	<b>Slice #</b>	<b>Date Taken</b>
29	HL60	14	7/16/08

## U937 Cell Line – Cell #33

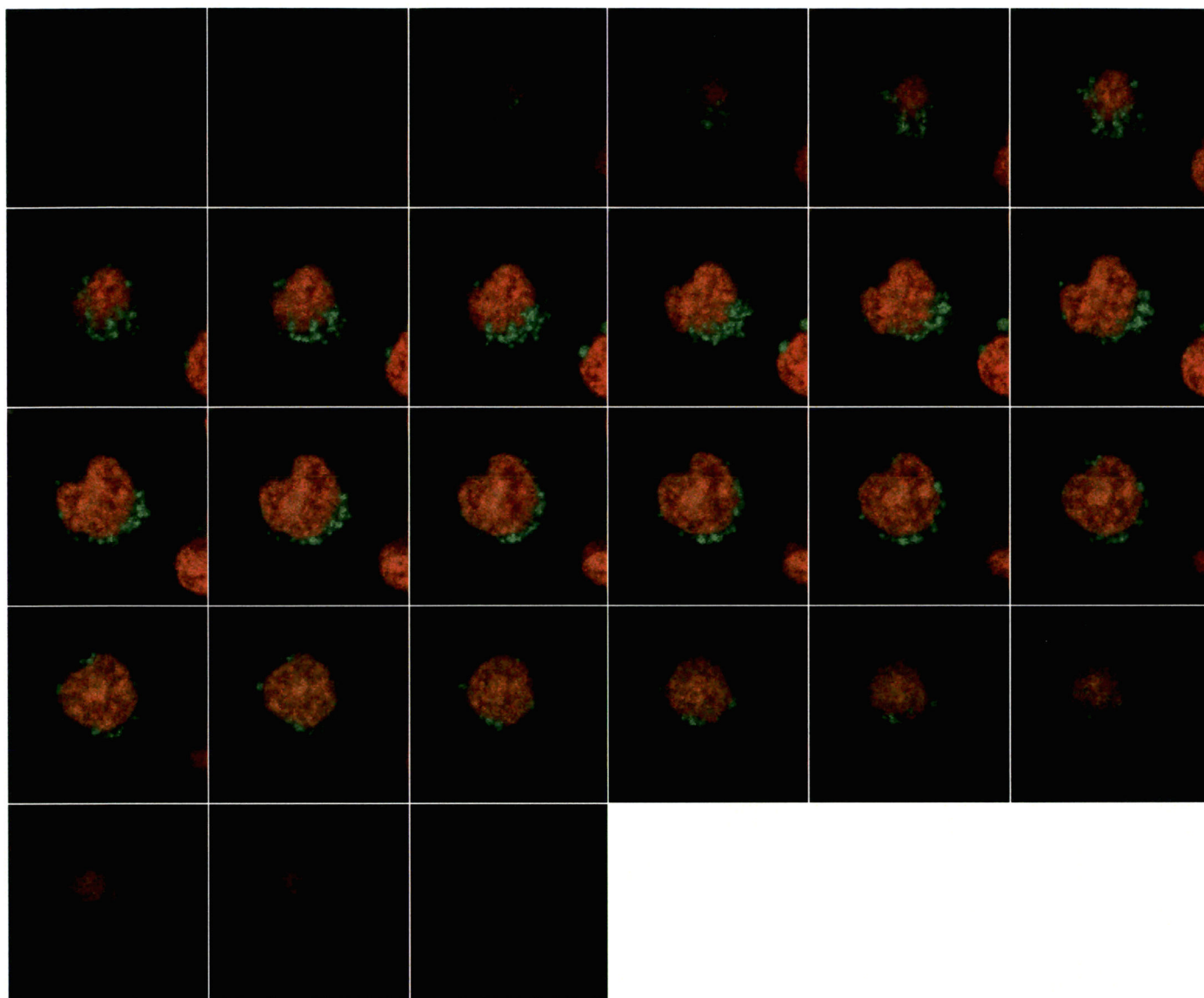
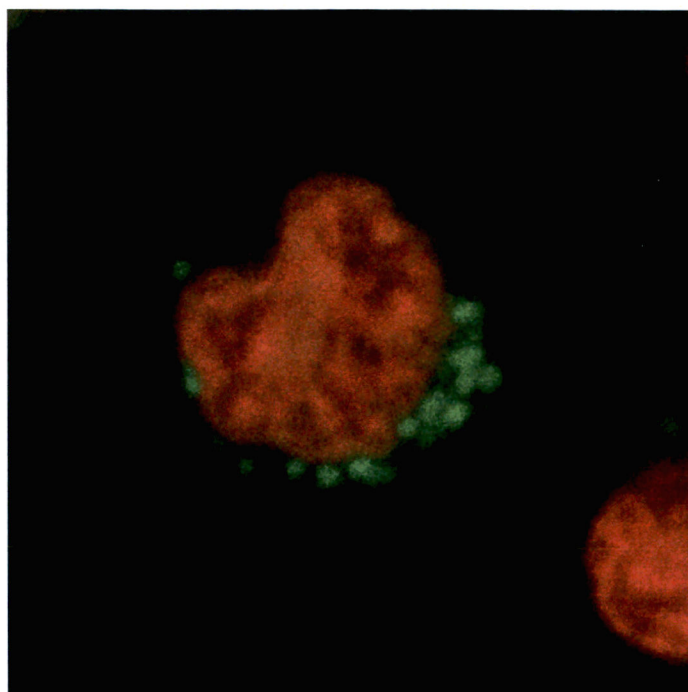
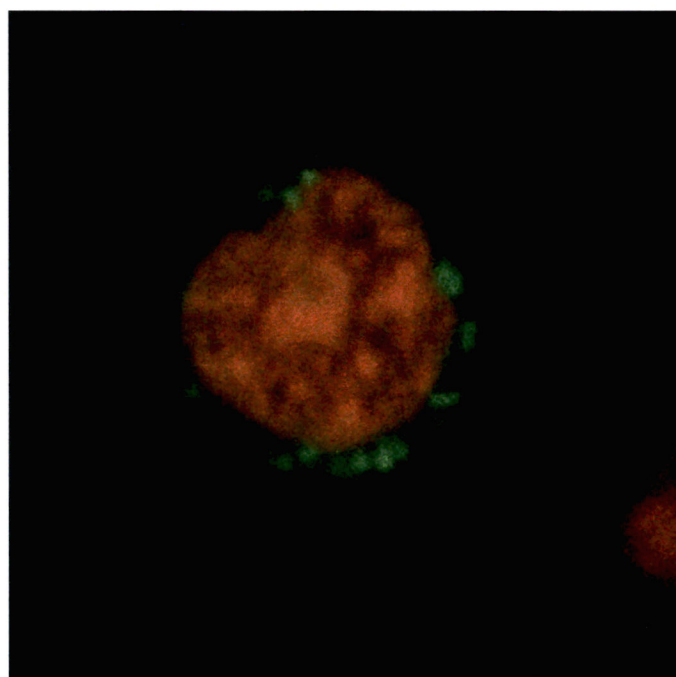


Image #	Date Taken	Saved As	Cell Morphology	Cell Diameter (um)	Nuclear Morphology	Mitochondria Morphology
33	7/16/2008	U937 #13	Round	12.5	Kidney, granular	Clustered beside nucleus

**U937 Cell Line – Cell #33**

<b>Image #</b>	<b>Cell Line</b>	<b>Slice #</b>	<b>Date Taken</b>
33	U937	13	7/16/08



<b>Image #</b>	<b>Cell Line</b>	<b>Slice #</b>	<b>Date Taken</b>
33	U937	18	7/16/08

## U937 Cell Line – Cell #34

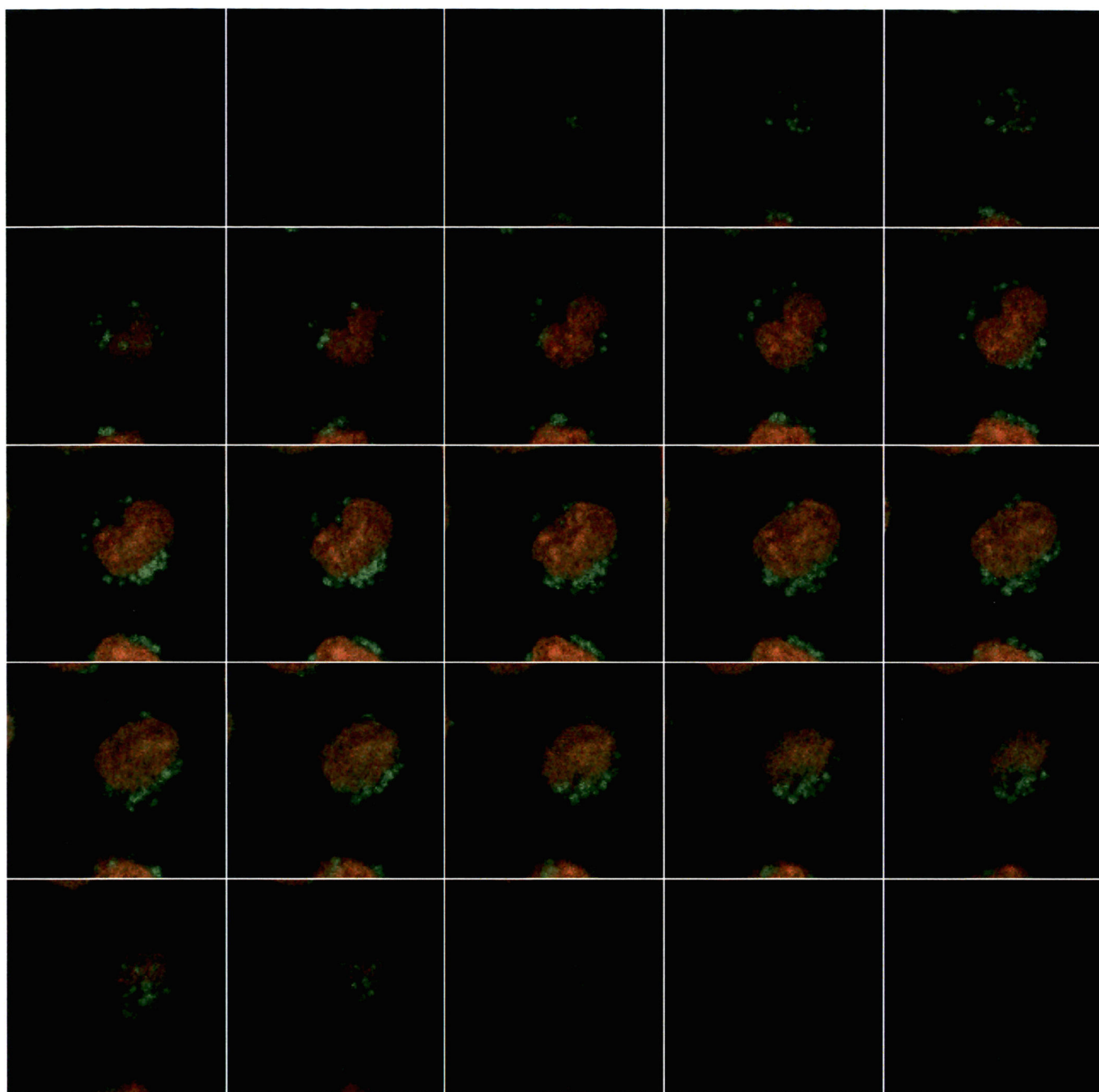
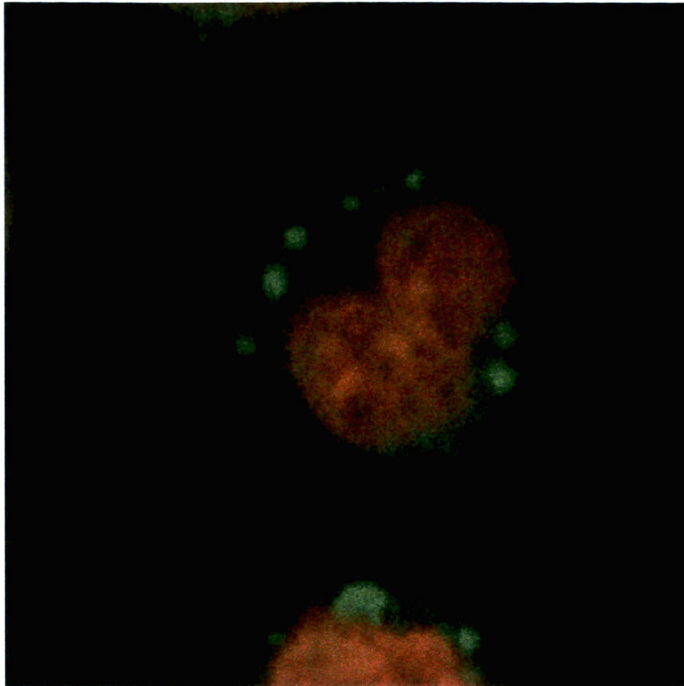
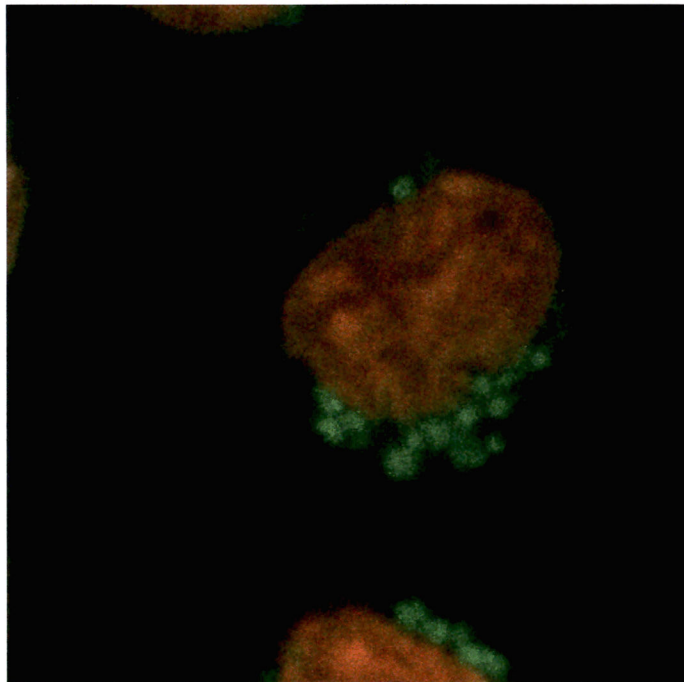


Image #	Date Taken	Saved As	Cell Morphology	Cell Diameter (um)	Nuclear Morphology	Mitochondria Morphology
34	7/16/2008	U937 #14	Round	11.5	Irregular, lobed, granular	Clustered around nucleus

**U937 Cell Line – Cell #34**

<b>Image #</b>	<b>Cell Line</b>	<b>Slice #</b>	<b>Date Taken</b>
34	U937	9	7/16/08



<b>Image #</b>	<b>Cell Line</b>	<b>Slice #</b>	<b>Date Taken</b>
34	U937	14	7/16/08

### Acute Lymphoid Leukemia Patient Cells – Patient #1, Cell #14

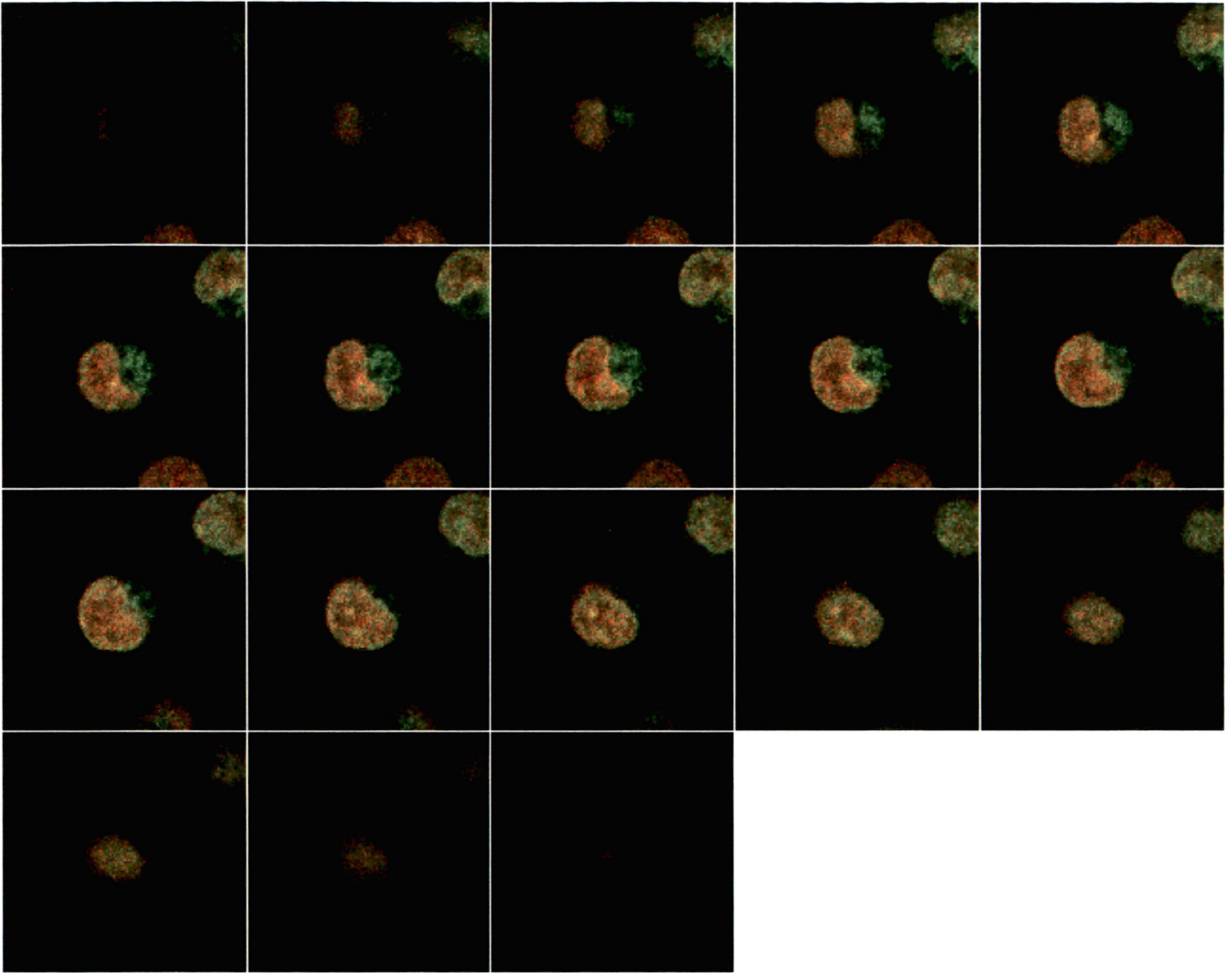


Image #	Date Taken	Saved As	Cell Morphology	Cell Diameter (um)	Nuclear Morphology	Mitochondria Morphology
14	4/11/2008	ALL 4	Round	8.5	Kidney, granular	Clustered beside nucleus

**Acute Lymphoid Leukemia Patient Cells – Patient #1, Cell #14**

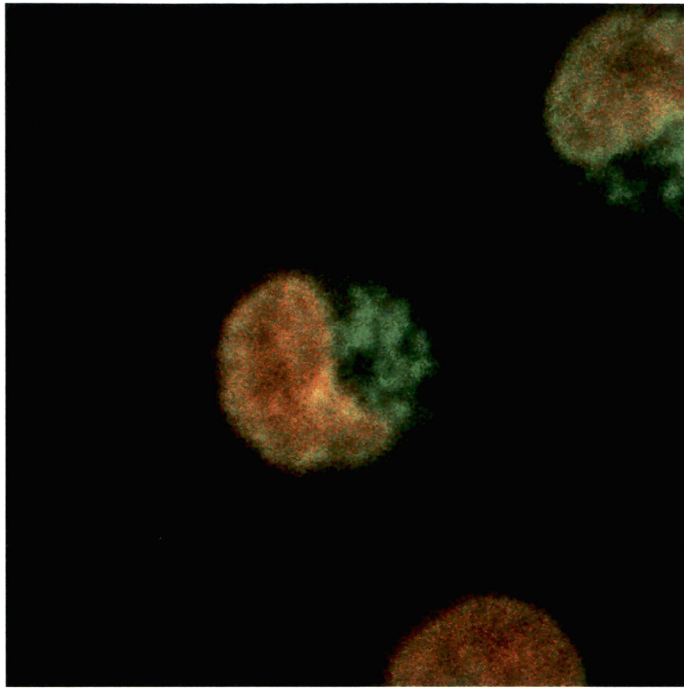


Image #	Cell Line	Slice #	Date Taken
14	Patient #1	6	4/11/08

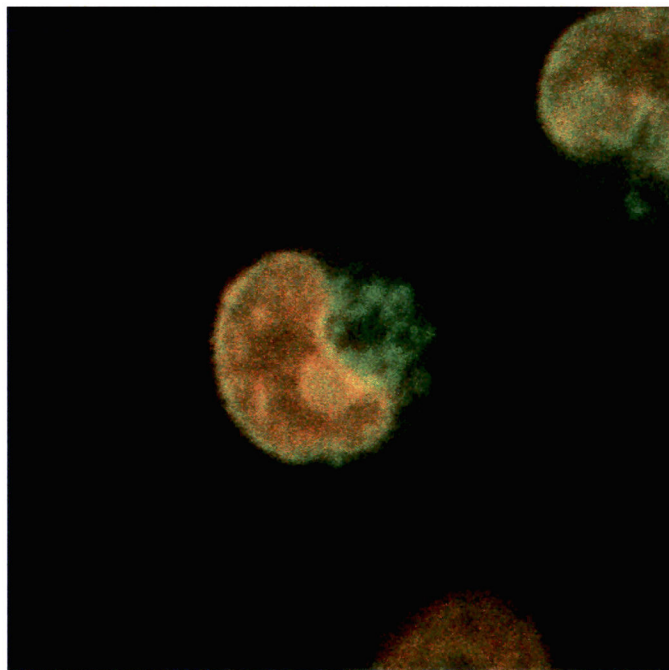


Image #	Cell Line	Slice #	Date Taken
14	Patient #1	9	4/11/08

### Acute Myeloid Leukemia Cells – Patient #5, Cell #16

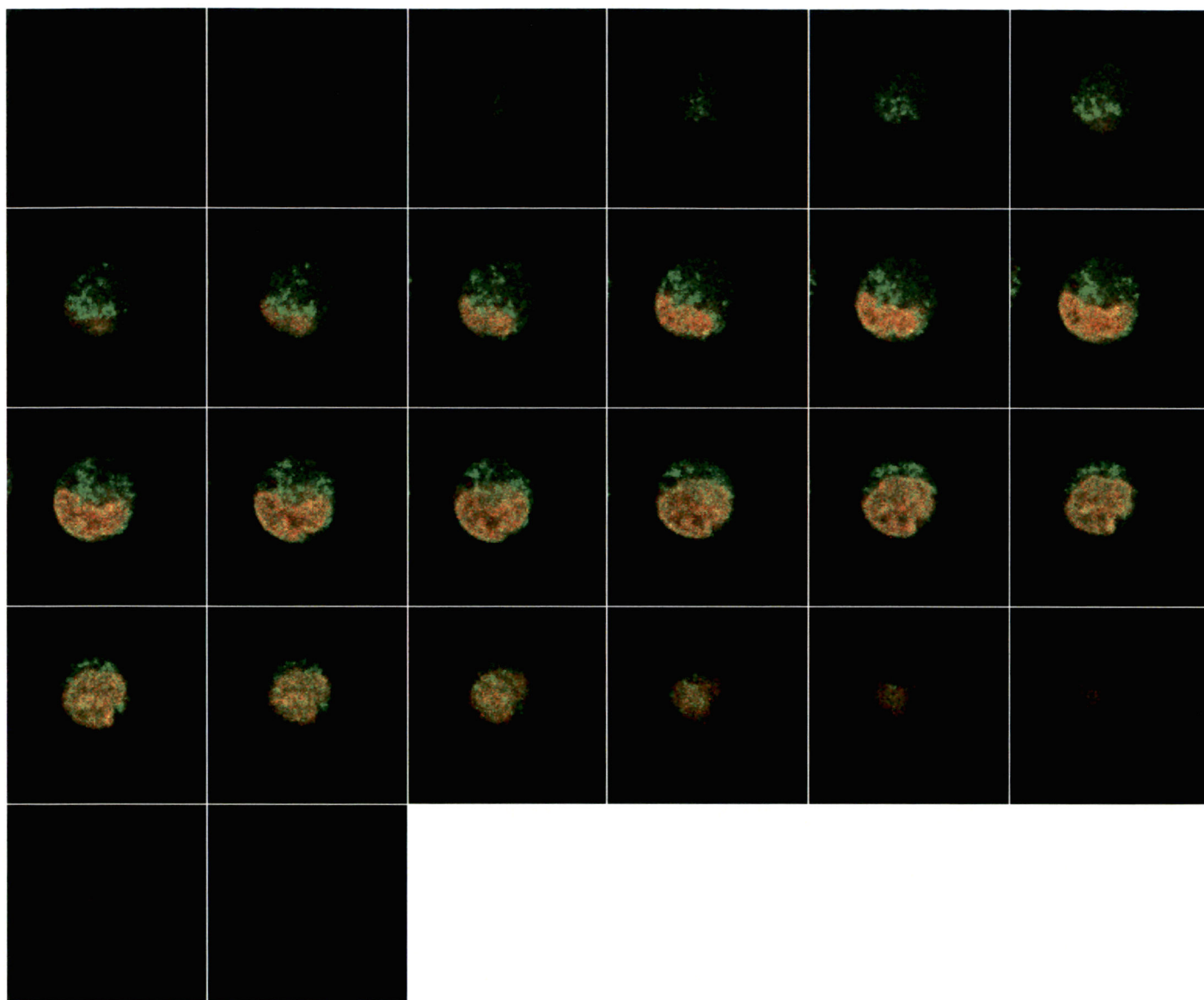
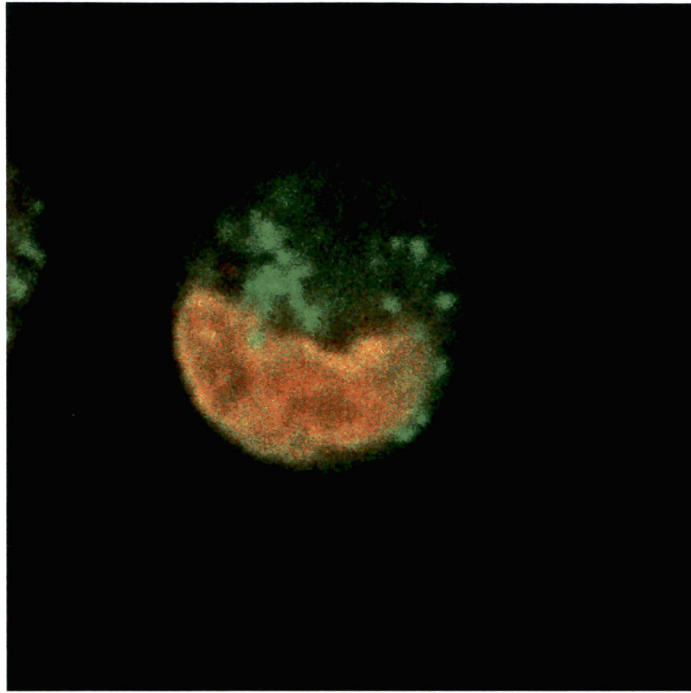
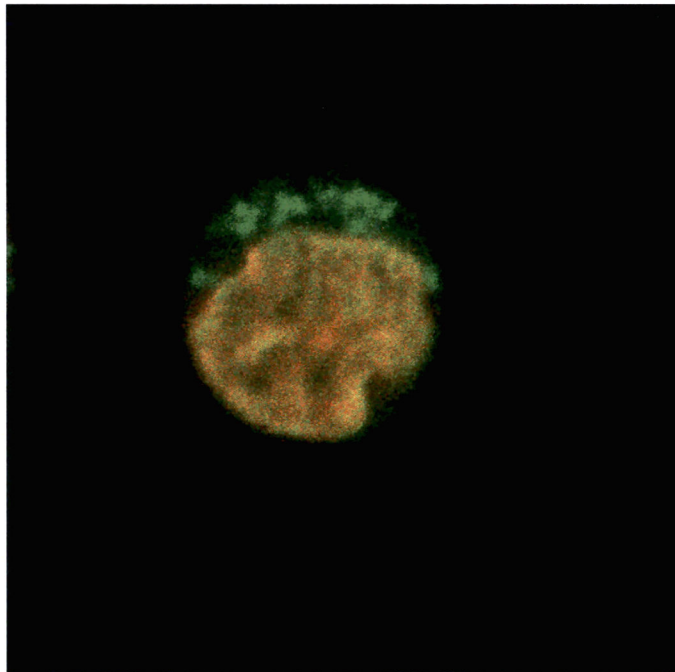


Image #	Date Taken	Saved As	Cell Morphology	Cell Diameter (um)	Nuclear Morphology	Mitochondria Morphology
16	7/21/2008	P5 #15	Round	10.0	Irregular, lobed, granular	Clustered above/beside nucleus

**Acute Myeloid Leukemia Cells – Patient #5, Cell #16**

<b>Image #</b>	<b>Cell Line</b>	<b>Slice #</b>	<b>Date Taken</b>
16	Patient #5	12	7/21/08



<b>Image #</b>	<b>Cell Line</b>	<b>Slice #</b>	<b>Date Taken</b>
16	Patient #5	17	7/21/08

### Undiagnosed Patient Cells – Patient #3, Cell #8

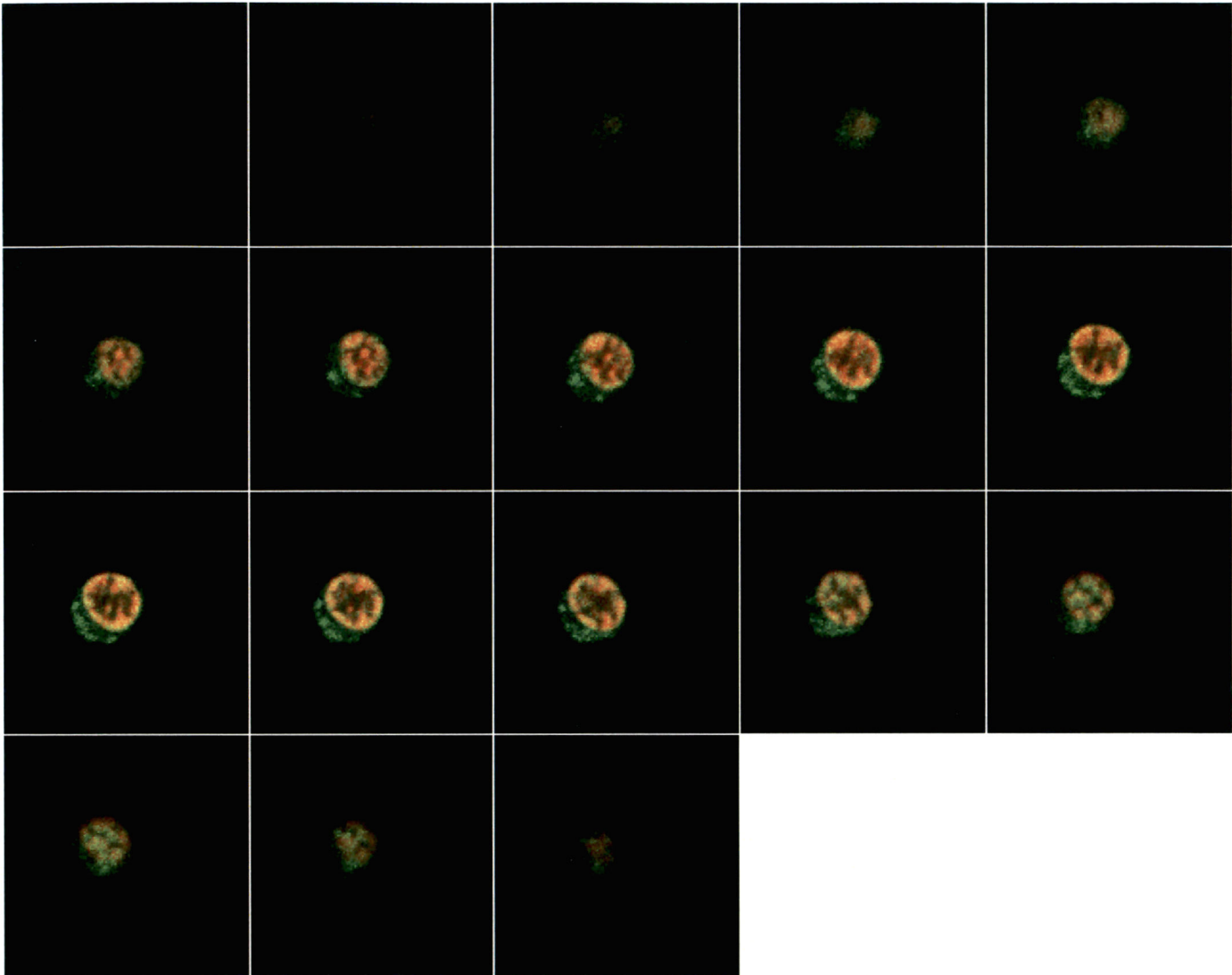
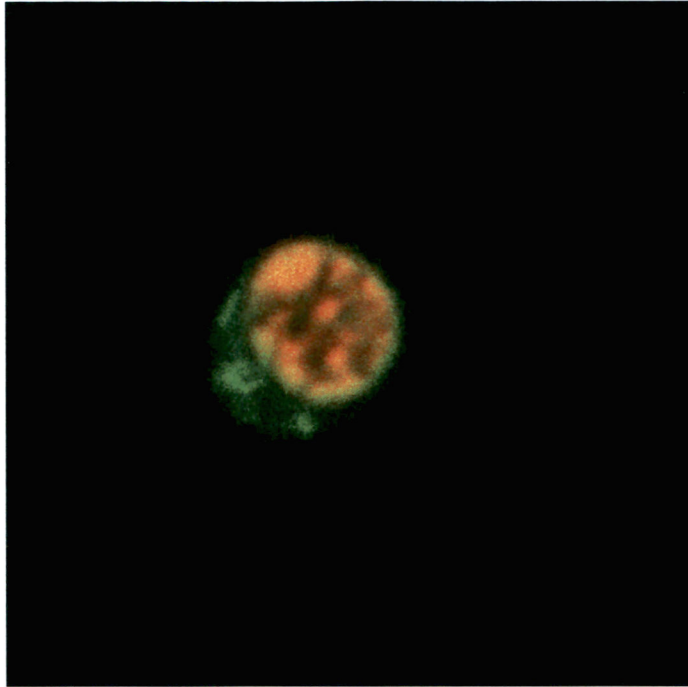
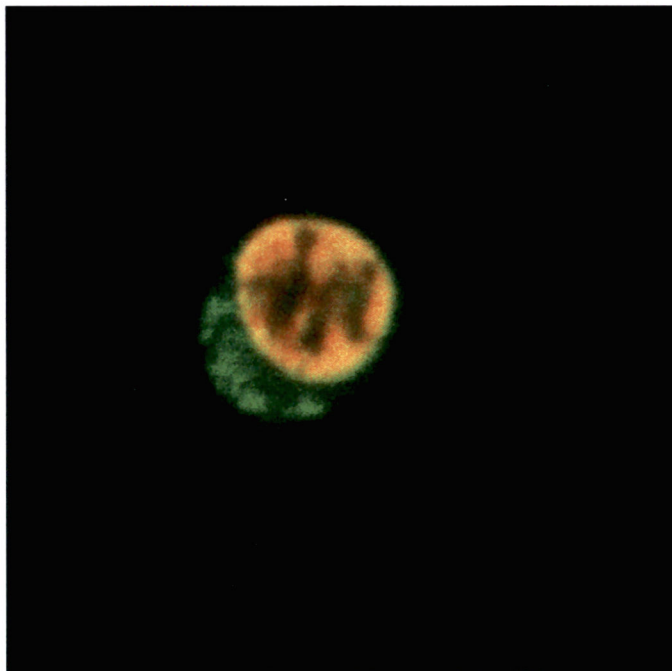


Image #	Date Taken	Saved As	Cell Morphology	Cell Diameter (um)	Nuclear Morphology	Mitochondria Morphology
8	6/20/2008	P3 #8	Oval	N/A	Round, granular	Clustered beside/below nucleus

**Undiagnosed Patient Cells – Patient #3, Cell #8**

<b>Image #</b>	<b>Cell Line</b>	<b>Slice #</b>	<b>Date Taken</b>
8	Patient #3	8	6/20/08



<b>Image #</b>	<b>Cell Line</b>	<b>Slice #</b>	<b>Date Taken</b>
8	Patient #3	10	6/20/08